INCLUSION OF FRACTURE SKIN IN DUONG'S MODEL OF RATE-DECLINE ANALYSIS FOR FRACTURE-DOMINATED SHALE RESERVOIRS

A Thesis

Presented to

the Faculty of the Department of Petroleum Engineering

University of Houston

In Partial Fulfillment

of the Requirements for the Degree

Master of Science

in Petroleum Engineering

By

Himanshu Shekhar Jha

December 2016

INCLUSION OF FRACTURE SKIN IN DUONG'S MODEL OF RATE-DECLINE ANALYSIS FOR FRACTURE-DOMINATED SHALE RESERVOIRS

Himanshu Shekhar Jha

Approved:

Chair of the Committee
Dimitrios G. Hatzignatiou, Professor
Petroleum Engineering, University of Houston

Committee Members:

Advisor, William John Lee, Professor
Petroleum Engineering, Texas A&M University

Konstantinos Kostarelos, Associate Professor
Petroleum Engineering, University of Houston

Suresh K. Khator, Associate Dean
Cullen College of Engineering
University of Houston

Mohamed Soliman, Department Chair
Petroleum Engineering
University of Houston

Acknowledgements

First and foremost, I want to thank my advisor Dr. John Lee for accepting me as his thesis student. It has been an absolute honor to be his student. He has taught me, both consciously and subconsciously, on how to think about solving any problem. I appreciate all his time, ideas and efforts which made my thesis experience productive and simulating.

I would also like to express my gratitude towards Dr. Dimitrios G. Hatzignatiou and Dr. Konstantinos Kostarelos for taking time out of their busy schedule to be on my defense committee.

Special thanks to Mohamed Khoshghadam for being a good friend and colleague. His support in getting the simulated data using IHS Harmony software along with his continuous feedback on my work was very helpful.

Finally, I am immensely grateful to parents and sisters who have always been my support and source of inspiration.

INCLUSION OF FRACTURE SKIN IN DUONG'S MODEL OF RATE-DECLINE ANALYSIS FOR FRACTURE-DOMINATED SHALE RESERVOIRS

An Abstract

of a

Thesis

Presented to

the Faculty of the Department of Petroleum Engineering

University of Houston

In Partial Fulfillment

of the Requirements for the Degree

Master of Science

in Petroleum Engineering

By

Himanshu Shekhar Jha

December 2016

Abstract

Production forecast plays an important role in helping us make rational decisions in face of large uncertainties. Unconventional oil and gas production has followed an accelerated growth trajectory in the US oil and gas industry. Unconventional reservoirs vary significantly in their reservoir characteristics and production methodologies when compared to conventional reservoirs. The differences between conventional and unconventional reservoirs lead to significant durations of transient flow regimes for the unconventional reservoirs and this calls for using new methodologies for reserves forecast.

Work by Valko and Lee (SPE 134231), and Duong (SPE 137748) are some of the most popular methods of decline curve analysis for unconventional reservoirs. This thesis presents a critique of Duong's Method for rate decline analysis for fracture-dominated shale reservoir and proposes a more rigorous method for reserve forecast by including fracture skin in Duong's model. The proposed new method can be used for unconventional oil and gas reservoirs.

Table of Contents

List of Figures

List of Tables

1 Introduction

Growth in U.S. oil and gas resource (proved and technically recoverable resources) and cumulative production has averaged 1.8% and 2.5% per year for crude oil and natural gas, respectively, from 1995-2005, and 3.6% per year and 3.1% per year from 2005-2015. The reason for this increase can be attributed to improved production from unconventional resources. Technological improvements such as better rigs and drill bits that can drill well faster at lower unit costs, improved hydraulic fracturing techniques that expose more of reservoir to the well, better control of drill bit path, and better offshore rigs and platforms that can reach great depths and handle extreme pressures and temperatures have contributed to the cost reductions. These technological improvements have allowed, and are likely to continue to allow, the expansion of tight and shale gas production as indicated in the figure 1.1(Annual Energy Outlook, 2016).

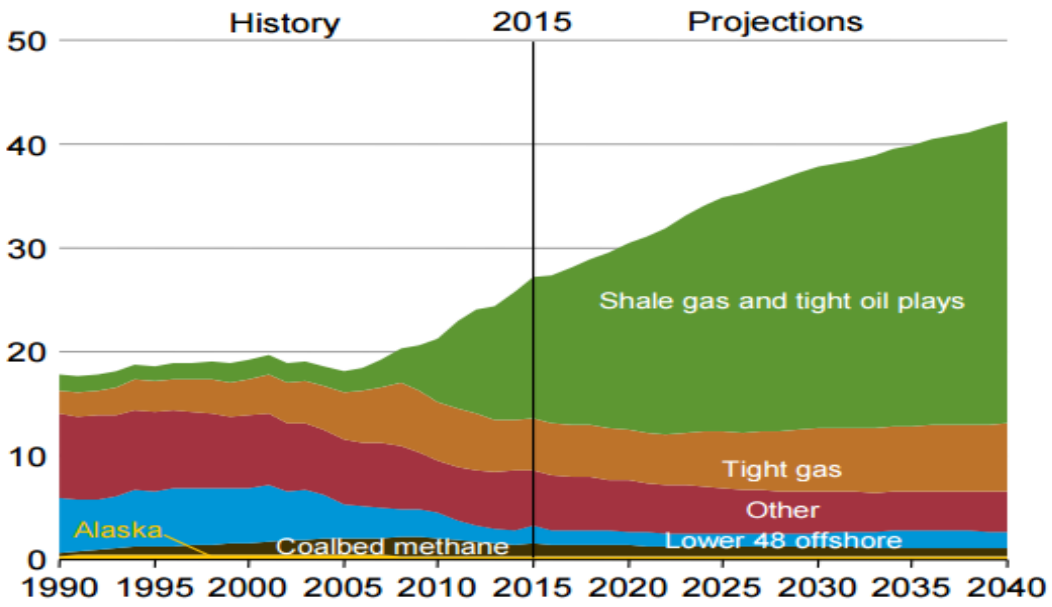

Figure 1.1: Prediction of shale gas and tight oil plays (Annual Energy Outlook, 2016)

Petroleum resources management system (PRMS) defines reserves as those quantities of petroleum anticipated to be commercially recoverable by application of development projects to known accumulations from a given date forward under defined conditions.

The four traditional methods of reserves estimation along with one relative newcomer are as follows (Wright, 2014):

1. Analogy
2. Volumetric
3. Material Balance
4. Decline Curves
5. Reservoir Simulation (the, relatively, newcomer)

Each of these methods has advantages and disadvantages and each can be applied independently. Each method utilizes a different set of input data from the others to arrive at the same result – recoverable reserves. Because of their mutual independence, these different techniques can be used to complement each other and cross-check the predicted reserve estimates.

1.1 Analogy

Analogy is one of the most widely used unsophisticated method of reserve calculation. A close-to-abandonment analogous field is taken as an approximate to the current fields or wells. Recovery factor, bbls per acre foot, estimated ultimate recovery (EUR) and resource plays for shale oil and gas plays being developed by horizontal wells are some of the most common parameters determined for the current fields or wells by comparison with analogous fields or wells (Wright, 2014).

1.2 Volumetrics

The volumetric estimate of oil-in-place is one of the most important methods of determining reserves. This method is very simple, requiring only well logs and some estimated parameters; it may become more complex, requiring use of core data, special core analysis, suits of many types of logs and apparently sophisticated computer programs.

The fundamental volumetric equation for oil reservoirs (in oil field units) is:

$$EUR = 7758 \frac{Ah\phi(1 - S_{wi})}{B_{oi}} RF, \quad (1)$$

where EUR is the estimated ultimate recovery (STB), A is the drainage area (acres), h is the average thickness of net pay (ft), ϕ is the average porosity (decimal), S_{wi} is the average initial water saturation (decimal), B_{oi} is the initial oil formation volume factor (RB/STB), RF is the recovery factor (decimal) and 7758 is conversion factor (bbls/acre-ft) (Wright, 2014).

1.3 Material Balance

As production and pressure data become available from a field, material balance calculations are a good way of calculating the reserves with reduced uncertainties. Traditional material balance has been used for several decades to determine original oil in place or original-gas-in-place in conventional reservoirs. It requires varying the average static reservoir pressure over time and the PVT fluid properties.

It assumes the reservoir to be hydrocarbon tank and uses law of conservation of mass to calculate original oil and/or gas in place and make predictions of future field performance.

The law of conservation of mass can be expressed as:

$$\begin{aligned} &mass\ produced \\ &\quad = mass\ originally\ in\ place \\ &\quad - mass\ currently\ in\ place. \end{aligned} \tag{2}$$

Equation 2 can be applied to each hydrocarbon component or the accumulation can be treated as single component (usually gas) or two components (oil and gas). Since we measure volume, not mass, the equation is usually expressed in terms of volume as:

$$\begin{aligned} &Volume\ Produced \\ &\quad = Volume\ originally\ in\ place \\ &\quad - Volume\ remaining. \end{aligned} \tag{3}$$

As long as the density at standard conditions of the hydrocarbon being produced does not change, the conversion from mass to volume is acceptable (Wright, 2014).

1.4 Decline Curves

Production decline curves are one of the oldest methods of predicting oil and gas reserves. Most of the decline curves are empirical in nature, and rely on uniform, lengthy production periods of wells producing under "constant" conditions. They are typically plots of producing rate vs. time or producing rate vs. cumulative production plotted on a semi-log or log-log paper and extrapolated to give an estimate of production vs. time. They do not required assumptions about any of the reservoir properties such as A, h, ϕ, S_w or RF; instead they make use of production history data (6 months to 10 years) which is readily available. Modern decline curves also make use of measured or estimated bottom hole flowing pressure.

Decline curves are easy to analyze and often yield good results when wells are producing under “constant” conditions. Their major disadvantage is their apparent simplicity. Since they are so simple to use and provide answers on a time basis, they are the most commonly used of reserve estimation. However, decline curves are not as simple as they appear to be. In fact, they should be considered as rate transient tests, more difficult to analyze than pressure-transient tests (Wright, 2014).

1.5 Reservoir Simulation

Reservoir simulation is usually not primarily used for reserves analysis. It is mainly used to determine the reservoir’s petrophysical properties by achieving a history match, and to make future predictions can be made if one feels confident about the achieved history match. However, there is no guarantee that even with a good match, prediction runs will be close to actual results as the simulation match results are non-unique in nature.

Reservoir simulation represents the reservoir as a system of large number of cells, all interconnected rather than representing the whole reservoir as one single cell in the material balance. The fluid flow equations are then used to calculate the flow between cells (Wright, 2014).

2 Decline Curve Models

2.1 Arp's Decline Model

Arp's decline curve has been extremely popular in the industry for oil and gas reserves estimation. Arp's decline model uses three parameters namely *b* called the *decline curve exponent*, *D* called *decline rate* and q_i the *stabilized rate at time = 0.* Arp's decline curves are commonly characterized by the value of *b*, decline curve exponent. Any *b* value between 0 and 1 gives a hyperbolic decline curve with two special cases those of exponential decline (b = 0) and harmonic decline (b = 1) (Arps, 1946).

Arp's equation for the three cases discussed above are shown below:

Exponential Decline,

$$q_t = q_i \exp(-Dt), \tag{4}$$

Hyperbolic Decline,

$$q_t = \frac{q_i}{(1+bD_it)^{\frac{1}{b}}}, \text{ and} \tag{5}$$

Harmonic Decline,

$$q_t = \frac{q_i}{1+bt}, \tag{6}$$

Where b is one for harmonic decline, and q_t represents production rate at time t.

The exponential form of Arp's equation can be derived (Fetkovich et al., 1996) for systems with low compressibility (slightly compressible fluids) under certain conditions, most importantly

a) Constant bottom hole pressure, and

b) Stabilized (boundary-dominated) flow.

Arp's decline model assumes that b value remains constant for the entire flow period. In case of unconventional reservoirs with permeability ranging from micro-Darcies to nano-Darcies, transient flow periods have b values greater than 1 (Maley,1985 and Spivey et al., 2001) decreasing significantly with time (Lee and Sidle, 2010).

With values of b greater than or equal to 1, it can be very easily shown that cumulative production is infinite for infinite producing time. This is not a physically meaningful result even when considering infinite production time. Thus, reserves must not be estimated by extrapolating the curve for $b > 1$ to an abandonment rate.

In conclusion, Arp's Decline curve model should only be used when decline exponent is in the range (0,1) for a reservoir under boundary dominated flow under constant pressure production.

2.2 Duong's Production Decline Model

Duong's method is an empirical equation that is derived based on long-term transient flow in large number of unconventional reservoirs (Duong, 2011). Duong's method uses the following three equations for rate forecast, cumulative production forecast, and EUR calculations:

$$q_t = q_1 t^{-m} \exp\frac{a\,(t^{1-m}-1)}{1-m} + q_{\infty}, \tag{7}$$

$$G_P = \frac{q_1}{a} \exp\frac{a\,(t^{1-m}-1)}{1-m}, \text{ and} \tag{8}$$

$$EUR = \frac{q_{eco}}{a} t_{eco}^{m}, \tag{9}$$

where q_1 is the flow rate at time at 1 day, a, m, q_∞ are empirical constants defined by Duong in his model, q_{eco} is the minimum economic rate, and t_{eco} is the time at which $q = q_{eco}$.

The following sub-sections explain the derivation and the workflow of the Duong's method as outline in his paper (Duong, 2011).

2.2.1 Derivation of Duong's Method

Duong (2011) neglected the presence of fracture skin in the flowrate equation and wrote the flow rate at any time for a constant pressure drawdown as

$$q = q_1 t^{-n}, \tag{10}$$

where n is one-half for linear flow, n is one-quarter for bilinear flow, and q_1 is the flow rate at day 1.

Using equation 1, the gas cumulative volume at time t will be:

$$G_P = \int_0^t q(t)dt = q_1 \frac{t^{1-n}}{1-n}. \tag{11}$$

Using equations 10 and 11,

$$\frac{q}{G_P} = \frac{1-n}{t}. \tag{12}$$

However, while analyzing real field data from several shale-gas play to test equation 12, Duong found that a log-log plot of $\frac{q}{G_P}$ vs. time in days yields a straight line with a negative slope, $-m$, and an intercept of a (Duong, 2011).

That is,

$$\frac{q}{G_P} = at^{-m}. \tag{13}$$

In the field examples analyzed by Duong, m was found always greater than unity for shale reservoirs and any value of m less than 1 would indicate a conventional tight well. Based on these observations, the author developed the following general equation:

$$\frac{q}{G_P} = \epsilon(t). \tag{14}$$

Taking the derivative on both sides of equation 14 with respect to time, we have

$$\frac{d}{dt}[q/\epsilon(t)\,] = \frac{d}{dt}G_P. \tag{15}$$

Using $q' = dq/dt$ and $\epsilon'(t) = d\epsilon(t)/dt$ equation 15 becomes

$$\frac{q'}{\epsilon(t)} - \frac{q\epsilon'(t)}{\epsilon^2(t)} = q, \tag{16}$$

or

$$\frac{dq}{q} = \frac{d\epsilon(t)}{\epsilon(t)} + \epsilon(t)dt. \tag{17}$$

Integrating both sides of equation 17 from $t = 1\ day$ to $t = t\ days$, we have

$$\ln\left(\frac{q}{q_1}\right) = \ln\left(\frac{\epsilon(t)}{\epsilon(1)}\right) + \int_1^t \epsilon(t)dt, \tag{18}$$

where q_1 is the theoretical rate at t = 1 day.

Equation 18 gives us the expression for flow rate and cumulative production as

$$q = q_1 \frac{\epsilon(t)}{\epsilon(1)} \exp\left(\int_1^t \epsilon(t)dt\right), \tag{19}$$

which for equation 14 yields:

$$G_P = \frac{q_1}{\epsilon(1)} \exp\left(\int_1^t \epsilon(t)dt\right). \tag{20}$$

If,

$$\frac{q}{G_P} = at^{-m}, \text{ then} \tag{21}$$

$$\epsilon(t) = at^{-m}. \tag{22}$$

Equations 19, 20 and 21 can then be written as:

$$q_t = q_1 t^{-m} \exp \frac{a\,(t^{1-m} - 1)}{1-m}, \tag{23}$$

$$G_P = \frac{q_1}{a} \exp \frac{a\,(t^{1-m}-1)}{1-m}, \text{ and} \tag{24}$$

$$EUR = \frac{q_{eco}}{a} t_{eco}^{m}. \tag{25}$$

2.2.2 Workflow for Duong's Method (Lee, 2014)

Step1: Check and correct field production data.

- Identity the data in transient flow regime. Duong's method is only applicable to this part of data.
- Identify bad data (fracture fluid clean-up, uncorrected early data due to poor /no pressure measurement). Do not apply Duong's method to this part of data.

- Plot histories such as flowing WHP, gas rate and water rate vs. time and identify the non-idealities such as choked-back flow (rate increasing or constant, high WHP, flat rates).
- Correct (normalize) rates for changes in BHP using following equation:

$$q_{corr} = q_{obs}\frac{p_i - p_{wf,stabilized}}{p_i - p_{wf,obs}}. \quad (26)$$

- Correct wet-gas rates to equivalent dry-gas rates for high condensate/gas ratios.

Step 2: Determination of *a* and *m.*

- Construct a log-log plot of q/G_P (or q/N_P for oil) vs. time.
- Fit a straight line to the desired section of data determined in Step 1.
- Determine *a* from the intercept of the straight line, *m* from the slope of the straight line.

Step 3: Determination of q_1.

- Plot *q* vs *t(a m)* where

$$t(a,m) = t^{-m}\exp\frac{a\,(t^{1-m}-1)}{1-m}. \quad (27)$$

- This plot should yield a straight line passing through origin with slope equal to q_1(see equation 23).
- Duong suggests that intersection of line up or down from origin may be necessary to improve the fit, leading to non-zero intercept, q_∞. This gives the expression for q as:

$$q = q_1 t(a,m) + q_\infty \quad (28)$$

Step 4: Estimate future production, cumulative production, and EUR from equation 23, 24 and 25 respectively.

3 Critique of Duong's Model & Work Objectives

3.1 Critique of Duong's model

3.1.1 Fracture skin

In his formulation, Duong ignored the presence of fracture skin and wrote the rate equation as:

$$q(t) = q_1 t^{-n}. \tag{29}$$

Therefore, the cumulative gas will be:

$$G_P(t) = \int_0^t q dt = \frac{q_1 t^{1-n}}{1-n}, \tag{30}$$

and the ratio of flow rate to cumulative gas production can be expressed as:

$$\frac{q}{G_P} = \frac{1-n}{t}. \tag{31}$$

The above expression is a mathematically rigorous expression that when plotted between q/G_P vs. time on a log-log plot should give a straight line with slope -1. Instead, Duong used the following empirical expression which provided him a better "fit" for real field data:

$$\frac{q}{G_P} = a t^{-m}. \tag{32}$$

Comparing equations 31 and 32, one can expect the value of a to be equal to $(1-n)$ and value of m to be -1. However, Duong observed that for shale reservoirs 'm' always has a value greater than 1, and he also suggested that any value of m less than unity may indicate a conventional tight well.

We believe that Duong did not "observe" the $\frac{q}{G_P} = \frac{1-n}{t}$ relationship in the real field data because he ignored the presence of fracture skin, which is present in most of the hydraulic fractures.

3.1.2 Inconsistent dimensions

Duong presented an empirical relationship between daily production (q) and cumulative production (G_P) as shown in equation 32. The ratio, q/G_P should always have a dimension of $[t]^{-1}$, however the proposed empirical equation gives the dimension of this ratio as $[t]^{-m}$. As shown by Duong's work, m can have values greater and smaller than 1 which destroys the dimensional sanctity of this equation.

This error in the dimension of this ratio is carried forward in all the equations derived for use in Duong's model. The flow rate (q) and cumulative production (G_P), as shown in equations 23 and 24, have units of $[L]^3[t]^{-(1+m)}$ and $[L]^3[t]^{-1}$.

We believe that the Duong's model does not account for the fracture skin in the rate calculation which forces him to use the proposed empirical expression.

3.1.3 Unbounded reserves for $m \leq 1$

The G_P expression derived by Duong fails to present bounded reserve calculation for values of m less than or equal to 1. As shown in equation 13, the empirical form assumed by Duong's model is:

$$\frac{q}{G_P} = at^{-m}. \tag{33}$$

Using $q = dG_P/dt$ in equation 33,

$$\frac{\frac{dG_p}{dt}}{G_P} = at^{-m}. \tag{34}$$

Separating the variable in equation 34 gives us,

$$\frac{dG_p}{G_P} = at^{-m}dt. \tag{35}$$

Integrating equation 35 from 0 to t gives the gas reserve expression as:

$$G_P = G_{Pi} \exp(\frac{at^{1-m}}{1-m}), \tag{36}$$

where G_{Pi} is the initial reserve at time $t = 0$.

It can be seen from this expression of reserves calculation that for $m = 1$, the expression for G_P is not defined and for any $m < 1$, reserves would be increasing with time which is physically impossible. In his work, Duong suggested that it is possible to get cases with $m < 1$ for conventional tight wells.

3.1.4 Non-monotonic *t(a,m)* function

Duong model derives the expression for flowrate as shown in equation 23 as:

$$q = q_1 t^{-m} e^{\frac{a(t^{1-m}-1)}{1-m}}, \tag{37}$$

where q_1 is the flow rate at 1 day.

To determine the value of q_1, Duong proposed to plot a graph between flowrate (q) and the function $t(a,m)$ where $t(a,m)$ is given by following equation:

$$t(a,m) = t^{-m} e^{\frac{a(t^{1-m}-1)}{1-m}}. \quad (38)$$

Duong's model believes that q is directly proportional to $t(a,m)$ and a graph between the two would result in a straight line with slope q_1.

Our work shows that q is not directly proportional to $t(a,m)$ and trying to fit a straight line to obtain the value of q_1 will result in some errors.

For constant pressure drawdown, we know that flowrate (q) is inversely proportional to time (t). As we believe that flowrate q is directly proportional to $t(a,m)$, the function $t(a,m)$ should also be inversely proportional to time. This means that $t(a,m)$ should monotonically decrease with increasing time. In terms of derivative this would mean that:

$$\frac{dt(a,m)}{dt} < 0. \quad (39)$$

The derivative of *t(a,m)* with respect to time is given by:

$$\frac{dt(a,m)}{dt} = (at^{1-m} - m)t^{-(1+m)} e^{\frac{a(t^{1-m}-1)}{1-m}}. \quad (40)$$

The sign of this derivative expression would be determined by the sign of the $(at^{1-m} - m)$ as the rest of the terms in the derivative expression (equation 40) are non-negative. It can be seen that

$$at^{1-m} - m < 0 \; for \; t < \left(\frac{m}{a}\right)^{\frac{1}{1-m}}, and \quad (41)$$

$$at^{1-m} - m > 0 \; for \; t > \left(\frac{m}{a}\right)^{\frac{1}{1-m}}. \quad (42)$$

It should be noted that $(at^{1-m} - m)$ changes its sign at $t = \left(\frac{m}{a}\right)^{\frac{1}{1-m}}$. Therefore, $t(a, m)$ is not monotonically decreasing with time and a graph between $q(t)$ and $t(a, m)$ will not be linear. Instead the graph will show an inflection point at $t = \left(\frac{m}{a}\right)^{\frac{1}{1-m}}$ hours. Trying to fit a straight line for this case will result in some errors in the determination of q_1.

3.1.5 Error in cumulative production calculation

As stated in the previous point, Duong suggested using a graph between $q(t)$ and $t(a, m)$ to determine the value of q_1. The straight line fitted between $q(t)$ and $t(a, m)$ should pass through the origin to give the slope as q_1.

However, Duong noticed that the "best fit" for the real data did not give a line passing through the origin and modified the new expression for $q(t)$ as follows:

$$q(t) = q_1 t(a, m) + q_\infty, \tag{43}$$

where q_∞ is rate the at infinite time, so it could be zero, negative, or positive. This addition of q_∞ to the $q(t)$ calculation introduces another error.

We know that,

$$G_P(t) = \int_0^t q(t)dt. \tag{44}$$

Using equation 43 for the calculation of cumulative production,

$$G_P(t) = \int_0^t (q_1 t(a, m) + q_\infty)dt. \tag{45}$$

As, q_∞ is constant and does not change with time, it can be taken out of integral. That gives the cumulative production as follows:

$$G_P(t) = \int_0^t q_1 t(a,m)dt + q_\infty t. \quad (46)$$

As it can be seen in the above expression, $G_P(t)$ is reduced or increase by additional amount of $q_\infty t$ which is not correct.

3.2 Objectives of this study

The objective of this study is to present a critique of the Duong's model for rate decline analysis for fracture dominated shale reservoir and develop a new decline curve model which is mathematically more sound and rigorous.

Section 6 will discuss the derivation and work-flow of new decline curve analysis model. The new decline curve analysis model will be derived from the transient flow equations and will be referred as modified Duong model from this point on.

Section 7 and 8 will present the comparison of prediction results from the Duong model and modified Duong model for the flow rate and cumulative production calculated using analytical equations and numerical modelling respectively.

4 Fracture Damage

There are two proposed models for fracture damage (Cinco and Samaniego, 1981); (a) the choke fracture damage model and (b) the fracture face damage skin model.

4.1 Chocked fracture damage skin model

In a chocked fracture damage skin factor model, the portion near the wellbore is damaged as shown in figure 5.1.

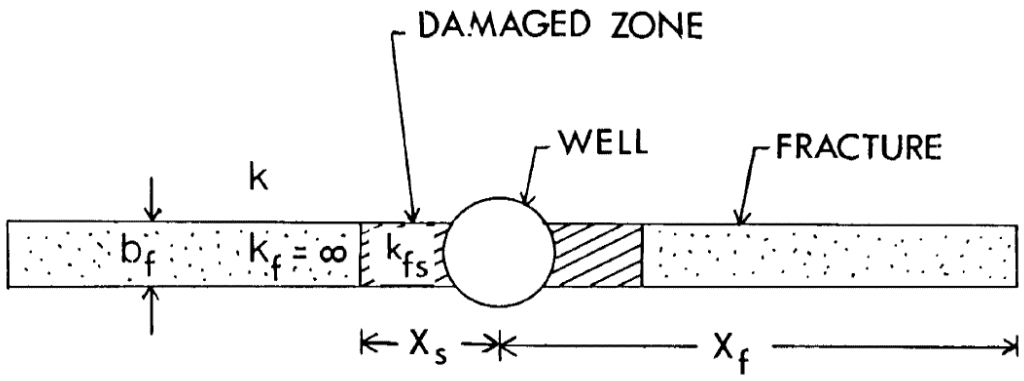

Figure 4.1: Chocked fracture face damage skin model (Cinco and Samaniego, 1981)

Reasons for having a chocked fracture damage include proppant crushing or embedment because of excessive stress, over flushing of proppant pushing the proppant pack away from the well, and producing back proppant leaving the near-wellbore portion of the fracture unpropped (Spivey and Lee, 2013).

The skin factor caused by chocked fracture may be calculated by using the formula given by (Cinco and Samaniego, 1981):

$$S_f = \frac{\pi k X_s}{(wk_f)_d}, \tag{47}$$

where S_f is the chocked fracture damage skin, k is the reservoir permeability, X_s is the length of damage inside fracture, $(wk)_d$ equals to the width of fracture times the damaged fracture permeability.

4.2 Fracture face damage skin factor model

In the fracture face damage skin factor model, the formation permeability adjacent to the fracture face is damaged as shown in figure 5.2.

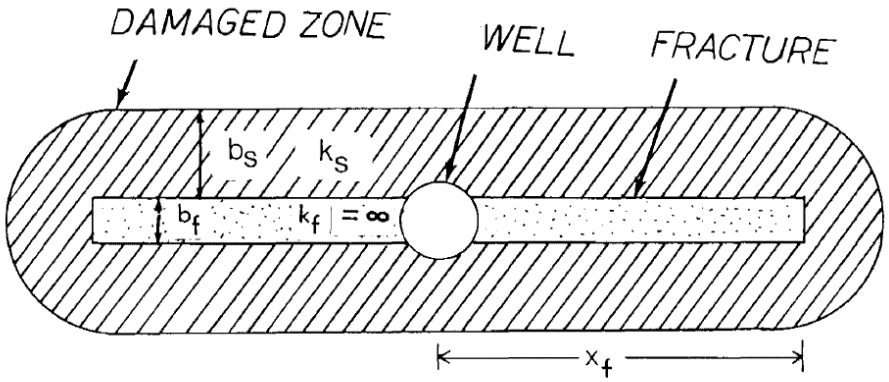

Figure 4.2: Fracture face damage skin factor model (Cinco and Samaniego, 1981)

In the fracture face damage skin factor model, the formation permeability is reduced to k_s within a distance b_s around the fracture, which may be caused due to reaction of fracture fluid with the formation water (Spivey and Lee, 2013).

The fracture face damage skin factor may be calculated using following formula (Cinco and Samaniego, 1981):

$$S_f = \frac{\pi b_s}{2x_f}\left(\frac{k}{k_s} - 1\right), \tag{48}$$

where S_f is the fracture face damage skin factor, b_s is the width of damage zone around the fracture face, x_f is the fracture half-length, k is the matrix permeability, k_s is the damaged permeability around the fracture.

The effect of fracture face damage skin on pressure response for an infinite conductivity fracture is like that for chocked fracture skin. It is unlikely that the two cases may be distinguished from the real field data.

5 Modified Duong Method

Transient pressure drawdown response during bilinear flow is given by:

$$p_{wf} = p_i - \frac{44.1qB\mu}{h\sqrt{wk_f}}\left(\frac{t}{\mu\phi c_t k}\right)^{\frac{1}{4}} - \frac{141.2qB\mu}{kh}s_f, \tag{49}$$

and for linear flow,

$$p_{wf} = p_i - 4.064\frac{qB}{hL_f}\left(\frac{\mu t}{k\phi c_t}\right)^{\frac{1}{2}} - \frac{141.2qB\mu}{kh}s_f, \tag{50}$$

where p_{wf} is the bottomhole pressure (psi), p_i is the initial pressure (psi), q is the flow rate in bbl/day, B denotes the oil or gas formation volume factor, μ is the fluid viscosity (cP), h is the height of reservoir (ft.), w is the width of fracture, k_f is the fracture permeability (mD), ϕ is the porosity, c_t is the total formation compressibility (psi^{-1}), k is the reservoir permeability (mD), L_f is the fracture half-length, and S_f is the fracture skin.

Equations 49 and 50, for transient flow regime, can be rearranged as:

$$\frac{\Delta p}{q} = m_t t^n + b_t S_f, \tag{51}$$

where Δp is the pressure drawdown which equals to $(p_i - p_{wf})$, q is the flow rate, n is one half for linear flow, one quarter for bilinear flow, S_f is the fracture skin, m_t and b_t are constants dependent on fluid, reservoir, and facture properties given by table 6-1.

Table 5-1:'m_t' and 'b_t' values for linear and bilinear flow regime

Parameter	Bilinear flow	Linear flow
m_t	$\frac{44.1B\mu}{h\sqrt{wk_f}}\left(\frac{1}{\mu\phi c_t k}\right)^{\frac{1}{4}}$	$\frac{4.064B}{hL_f}\left(\frac{\mu t}{k\phi c_t}\right)^{\frac{1}{2}}$
b_t	$\frac{141.2B\mu}{kh}$	$\frac{141.2B\mu}{kh}$

The proposed generalized modified Duong model, when Δp value is known, is:

$$q(t) = \frac{\Delta p}{m_t t^n + b_t S_f}, \tag{52}$$

and thus,

$$G_P = \int_{t_1}^{t_2} q(t)dt + G_p(t_1). \tag{53}$$

Substituting equation 52 in equation 53 yields:

$$G_P = \int_{t_1}^{t_2} \frac{\Delta p}{m_t t^n + b_t S_f} dt + G_p(t_1). \tag{54}$$

5.1 Limiting case: flow rate and cumulative production, $S_f = 0$

When $S_f = 0$, equation 52 becomes:

$$q(t) = \frac{\Delta p}{ut^n}, \tag{55}$$

and equation 53,

$$G_P(t) = \int_0^t q(t)dt. \tag{56}$$

Therefore, by substituting equation 55 in 56,

$$G_P(t) = \int_0^t \frac{\Delta p}{m_t t^n} dt. \tag{57}$$

Solving the integral and applying the integration limits,

$$G_P(t) = \frac{\Delta p t^{1-n}}{(1-n)m_t}. \tag{58}$$

Table 6-2 and 6-3 summarize the expression for flow rate and cumulative production for the limiting case when S_f is zero depending on the availability of pressure data.

Table 5-2: Flow rate and cumulative production expressions when $S_f = 0$ and Δp data is available

$q(t)$	$\frac{\Delta p}{m_t t^n}$
$G_P(t)$	$\frac{\Delta p t^{1-n}}{(1-n)m_t}$

Table 5-3: Flow rate and cumulative production expressions when $S_f = 0$ and Δp data is not available

$q(t)$	$\frac{1}{(m_t/\Delta p)t^n}$
$G_P(t)$	$\frac{t^{1-n}}{(1-n)(m_t/\Delta p)}$

5.2 Derivation for linear flow

Using equation 54 for linear flow ($n = 1/2$),

$$G_P = \int_{t_1}^{t_2} \frac{\Delta p}{m_t t^{1/2} + b_t S_f} dt + G_p(t_1). \tag{59}$$

Taking $\Delta p/m_t$ outside the integral in equation 59, we get,

$$G_P = \frac{\Delta p}{m_t} \int_{t_1}^{t_2} \frac{1}{t^{1/2} + c} dt + G_p(t_1), \tag{60}$$

where

$$c = \frac{b_t S_f}{m_t}. \tag{61}$$

Defining

$$I_1 = \int \frac{dt}{t^{0.5} + c}, \tag{62}$$

and making substitution $t = \alpha^2$ in equation 62, then

$$dt = 2\alpha d\alpha. \tag{63}$$

Substituting equation 63 in equation 62, one obtains:

$$I_1 = \int \frac{2\alpha d\alpha}{\alpha + c}. \tag{64}$$

Writing $\alpha = \alpha + c - c$ in the numerator of equation 64, we get:

$$I_1 = 2\int \frac{(\alpha + c - c) d\alpha}{\alpha + c}. \tag{65}$$

On further solving the equation 65,

$$I_1 = 2\int d\alpha - 2c\int \frac{d\alpha}{\alpha + c}. \tag{66}$$

After evaluating the integrals in equation 66,

$$I_1 = 2\big(\alpha - cln(\alpha + c)\big). \tag{67}$$

Substituting $\alpha = t^{0.5}$ in equation 67 yields:

$$I_1 = 2(\mathrm{t}^{0.5} - \mathrm{c}\times \ln(t^{0.5} + c)). \tag{68}$$

Using equations 60 and 68, the following expression for cumulative field production can be obtained:

$$G_P = \frac{2\Delta p}{m_t}\left[(\mathrm{t}_2^{0.5} - \mathrm{t}_1^{0.5}) - \mathrm{c}\ln\left(\frac{t_2^{0.5} + c}{t_1^{0.5} + c}\right)\right] + G_p(t_1). \tag{69}$$

Table 6-4 and 6-5 summarize the expression for flow rate and cumulative production under linear flow conditions when pressure values are and are not available, respectively.

Table 5-4:Expressions for flow rate and cumulative production under linear flow conditions when Δp data is available

$q(t)$	$\dfrac{\Delta p}{m_t t^{1/2} + b_t S_f}$
$G_P(t)$	$\dfrac{2\Delta p}{m_t}\left[(\mathrm{t}_2^{0.5} - \mathrm{t}_1^{0.5}) - \mathrm{c}\times\ln\left(\dfrac{t_2^{0.5} + c}{t_1^{0.5} + c}\right)\right] + G_p(t_1)$

Table 5-5: Expressions for flow rate and cumulative production under linear flow conditions when Δp data is not available

$q(t)$	$\dfrac{1}{(m_t/\Delta p)} * \dfrac{1}{t^{1/2} + c}$
$G_P(t)$	$\dfrac{2}{(m_t/\Delta p)}\left[(\mathrm{t}_2^{0.5} - \mathrm{t}_1^{0.5}) - \mathrm{c}\times\ln\left(\dfrac{t_2^{0.5} + c}{t_1^{0.5} + c}\right)\right] + G_p(t_1)$

5.3 Derivation for bilinear flow

Using equation 54 for bilinear flow (n=1/4),

$$\mathrm{G}_P = \int_{t_1}^{t_2} \frac{\Delta p}{m_t t^{1/4} + b_t S_f} dt + G_p(t_1). \tag{70}$$

Taking $\Delta p/m_t$ outside the integral in equation 70, we get:

$$G_P = \frac{\Delta p}{m_t} \int_{t_1}^{t_2} \frac{1}{t^{1/4} + c} dt + G_p(t_1), \tag{71}$$

where $c = b_t S_f/m_t$ as given in equation 61.

Defining

$$I_2 = \int \frac{dt}{t^{\frac{1}{4}} + c}, \tag{72}$$

and substituting $t = \alpha^4$ in equation 72 gives us:

$$dt = 4\alpha^3 d\alpha. \tag{73}$$

Using equation 73 in equation 72 yields:

$$I_2 = \int \frac{4\alpha^3 d\alpha}{\alpha + c}. \tag{74}$$

Writing $\alpha^3 = \alpha^3 - c^3 + c^3$ in the numerator of equation 74, we get:

$$I_1 = 4\int \frac{\alpha^3 - c^3 + c^3}{\alpha + c} d\alpha. \tag{75}$$

On further solving equation 75,

$$I_2 = 4\left\{\int (\alpha^2 - \alpha c + c^2) d\alpha - c^3 \int d\alpha /(\alpha + c)\right\}. \tag{76}$$

After evaluating the integrals in equation 76,

$$I_2 = 4\left\{\left(\frac{\alpha^3}{3} - \frac{c\alpha^2}{2} + c^2\alpha\right) - c^3\ln(c+\alpha)\right\}. \tag{77}$$

Substituting $\alpha = t^{1/4}$ in equation 77 yields:

$$\mathrm{I}_1 = 4\left\{\left(\frac{t^{3/4}}{3} - \frac{ct^{1/2}}{2} + c^2t^{1/4}\right) - c^3\ln\left(c+t^{1/4}\right)\right\}. \tag{78}$$

Using equations 71 and 78, one obtains:

$$G_P(t) = \frac{4\Delta p}{m_t}\left\{\left(\frac{t_2^{3/4} - t_1^{3/4}}{3} - c\frac{t_2^{1/2} - t_2^{1/2}}{2} + c^2(t_2^{1/4} - t_1^{1/4})\right) - c^3\ln\left(\frac{t_2^{1/4}+c}{t_1^{1/4}+c}\right)\right\} + G_p(t_1). \tag{79}$$

Table 6-6 and 6-7 summarize the expression for flow rate and cumulative production under bilinear flow conditions when pressure values are and are not available, respectively.

Table 5-6: Expressions for flow rate and cumulative production under bilinear flow conditions when Δp data is available

$q(t)$	$\dfrac{\Delta p}{m_t t^{1/4} + b_t S_f}$
$G_P(t)$	$\dfrac{4\Delta p}{m_t}\left\{\left(\dfrac{t_2^{3/4} - t_1^{3/4}}{3} - c\dfrac{t_2^{1/2} - t_2^{1/2}}{2} + c^2(t_2^{1/4} - t_1^{1/4})\right) - c^3\ln\left(\dfrac{t_2^{1/4}+c}{t_1^{1/4}+c}\right)\right\} + G_p(t_1)$

Table 5-7: Expressions for flow rate and cumulative production under bilinear flow conditions when Δp data is not available

$q(t)$	$\frac{1}{(m_t/\Delta p)} * \frac{1}{t^{1/4}+c}$
$G_P(t)$	$\frac{4}{\left(\frac{m_t}{\Delta p}\right)}\left\{\left(\frac{t_2^{3/4}-t_1^{3/4}}{3} - c\frac{t_2^{1/2}-t_2^{1/2}}{2} + c^2(t_2^{1/4}-t_1^{1/4})\right) - c^3 \ln\left(\frac{t_2^{1/4}+c}{t_1^{1/4}+c}\right)\right\} + G_p(t_1)$

5.4 Derivation for any value of power n

Using equation 54,

$$G_P = \int_{t_1}^{t_2} \frac{\Delta p}{m_t t^n + b_t S_f} dt + G_p(t_1). \tag{80}$$

Taking $\Delta p/m_t c$ out of the integration in equation 80, we get:

$$G_P = \frac{\Delta \mathrm{p}}{m_t c} \int_{t_1}^{t_2} \frac{1}{\left(\frac{t}{c^{1/n}}\right)^n + 1} dt + G_p(t_1), \tag{81}$$

where $c = \frac{b_t S_f}{m_t}$ as given in equation 61.

Defining

$$I_3 = \int \frac{1}{\left(\frac{t}{c^{\frac{1}{n}}}\right)^n + 1} dt. \tag{82}$$

Substituting $\frac{t}{c^{1/n}} = x$ in equation 75, we get:

$$I_3 = c^{1/n} \int \frac{1}{x^n + 1} dt, \tag{83}$$

or

$$I_3 = c^{1/n} \int (x^n + 1)^{-1} dx. \tag{84}$$

Substituting x with α and adding limits to the integral in equation 84, we get:

$$I_3 = c^{1/n} \int_0^x (\alpha^n + 1)^{-1} d\alpha + k_1. \tag{85}$$

Substituting α with $\alpha^{1/n}$ and changing the limits of integral accordingly

$$I_3 = c^{1/n} \int_0^x (\alpha + 1)^{-1} d(\alpha^{1/n}) + k_2, \text{ or} \tag{86}$$

$$I_3 = \frac{c^{1/\mathrm{n}}}{n} \int_0^x (\alpha + 1)^{-1} . \alpha^{1/n-1} d\alpha + k_3. \tag{87}$$

Replacing α with αx^n and changing the limits of the integral accordingly gives,

$$I_3 = \frac{c^{\frac{1}{n}}}{n} \int_0^1 (\alpha x^n + 1)^{-1} . \ (\alpha x^n)^{\,1/n-1} d(\alpha x^n) + k_4. \tag{88}$$

Since x is a constant, $d(x^n t) = x^n dt$. Using it in equation 88 yields:

$$I_3 = \frac{c^{\frac{1}{n}}}{n} \int_0^1 (\alpha x^n + 1)^{-1} . \ x^{1-n} . \alpha^{\,1/n-1} . x^n d\alpha + k_5. \tag{89}$$

On further simplification,

$$I_3 = \frac{x c^{\frac{1}{n}}}{n} \int_0^1 (\alpha x^n + 1)^{-1} . \ \alpha^{\,1/n-1} d\alpha + k_6, \text{ or} \tag{90}$$

$$I_3 = \frac{x c^{\frac{1}{n}}}{n} {}_2\mathrm{F}_1\left(1, \frac{1}{n}; \frac{1+n}{n}; -x^n\right) + k, \tag{91}$$

where ${}_2\mathrm{F}_1(a,b;c;z)$ is a hypergeometric function and k_i are the various integration constants at various steps.

Substituting $x = t/c^{\frac{1}{n}}$ in equation 84

$$I_3 = \frac{t}{n} {}_2\mathrm{F}_1\left(1, \frac{1}{n}; \frac{1+n}{n}; -\frac{t^n}{c}\right) + k. \tag{92}$$

Using equation 81 and 92,

$$G_P = \frac{\Delta p}{m_t c}\left[\frac{t_2}{n} {}_2\mathrm{F}_1\left(1, \frac{1}{n}; \frac{1+n}{n}; -\frac{{t_2}^n}{c}\right) - \frac{t_1}{n} {}_2\mathrm{F}_1\left(1, \frac{1}{\mathrm{n}}; \frac{1+n}{n}; -\frac{{t_1}^n}{c}\right)\right]. \tag{93}$$

As it can be seen from equation 86, it is not possible for us to find an exact expression for G_P for every value of n. In such cases, G_P can be calculated using numerical integration such as Reimann sum, trapezoidal rule, or Simpson's rule.

5.4.1 Numerical integration using Simpson's rule

A definite integral means calculation of area under the curve between two bounds (lower limit and upper limit). In cases where we do not have an exact analytical expression for an integral, numerical integration can be used.

Reimann function approximates the height of the graph by a constant function and trapezoidal rule uses a linear approximation to the graph. With Simpson's rule, we match quadratics (i.e. parabolas), instead of straight or slanted lines to the graph. When Δx is

small, this approximates the curve very closely and we can obtain an accurate numerical approximation of the definite integral.

The final form of Simpson's rule is:

$$\int_a^b f(x)dx \approx \frac{\Delta x}{3}\left(f(0)+4f(1)+2f(2)+4f(3)+2f(4)\right. \\ \left.+\cdots+2f(n-2)+4f(n-1)+f(n)\right), \tag{94}$$

where n is the number of intervals and it must be even and Δx is the interval size given by:

$$\Delta x = \frac{b-a}{n}. \tag{95}$$

The error bound associated with Simpson's rule is given by:

$$|E_S| \leq \frac{k(b-a)^5}{180n^4}, \tag{96}$$

where E_S is the error bound associated with using the Simpson's rule and k is the maximum value of fourth derivative of $f(x)$ over the interval $[a,b]$such that $|f''''(x)| \leq k$ for some real value of k.

Tables 6-8 and 6-9 summarize the expressions for the flow rate and cumulative production for any general exponent n in transient flow regime when pressure values are and are not available, respectively.

Table 5-8: Expressions for flow rate and cumulative production for any general 'n' when Δp data is available

$q(t)$	$\frac{\Delta p}{m_t t^n + b_t S_f}$
$G_P(t)$	$G_P(t_1) + \int_{t_1}^{t_2} \frac{\Delta p}{m_t t^n + b_t S_f}\, dt$ Note: Integral needs to be determined numerically.

Table 5-9: Expressions for flow rate and cumulative production for any general 'n' when Δp data is not available

$q(t)$	$\frac{1}{(m_t/\Delta p)t^n + (b_t S_f/\Delta p)}$
$G_P(t)$	$G_P(t_1) + \int_{t_1}^{t_2} \frac{1}{(m_t/\Delta p)t^n + (b_t/\Delta p)S_f}\, dt$ Note: Integral needs to be determined numerically.

5.5 Workflow for Modified Duong Method

5.5.1 Case 1: When Δp data is available

Step1: Check and correct data.

- Identity the data in transient flow regime. Duong's method is only applicable to this part of data.
- Identify bad data (fracture fluid clean-up, uncorrected early data due to poor/no pressure measurement). Don't apply Duong's method to this part of data.
- Plot histories such as flowing WHP, gas rate and water rate vs. time and identify the non-idealities such as choked-back flow (rate increasing or constant, high WHP, flat rates).
- Correct wet-gas rates to equivalent dry-gas rates for high condensate/gas ratios.

Step 2: Determination of n

- Construct a log-log plot between $\Delta p/q$ vs. $time$. The slope of this graph gives us the value of n. It should be noted that this graph will not show the

"actual" value of as the plot will be affected the by the presence of fracture skin. For longer time periods, when the effect of fracture skin becomes negligible, "actual" value of n can be determined from the graph.

- Alternatively, use pressure derivative on the rate and pressure history data to determine the value of n. This is the best way to determine the value of n as pressure derivate it not affected by the presence of skin.

Step 3: Determination of m_t and $b_t S_f$

- Construct a plot Cartesian of $\Delta p/q$ vs. t^n.
- Fit a straight line through this data.
- Slope of this line gives the value of m_t and $b_t S_f$ can be determined from the intercept of the line.

Step 4: Rate (q) and cumulative production (G_P) prediction

- If the $b_t S_f$ value calculated in the step 3 comes out to be zero, use the equation from table 6-2 to calculate the future rate and cumulative production.
- If the $b_t S_f$ value calculated in the step 3 comes out to be a non-zero number, use equations from table 6-4, 6-6, or 6-8 to calculate the future production and cumulative production depending on the value of n calculated in step 1.

5.5.2 Case 2 When Δp data is not available

Step1: Check and correct data.

- Identity the data in transient flow regime. Duong's method is only applicable to this part of data.
- Identify bad data (fracture fluid clean-up, uncorrected early data due to poor/no pressure measurement). Don't apply Duong's method to this part of data.
- Plot histories such as flowing WHP, gas rate and water rate vs. time and identify the non-idealities such as choked-back flow (rate increasing or constant, high WHP, flat rates).
- Correct wet-gas rates to equivalent dry-gas rates for high condensate/gas ratios.

Step 2: Determination of n

- Construct a log-log plot between $1/q$ vs. $time$. The slope of this graph gives us the value of n. It should be noted that this graph will not show the "actual" value of n as the pressure and flow rate will be affected the by the presence of fracture skin. For longer time periods, when the effect of fracture skin becomes negligible, "actual" value of n can be determined from the graph.

Step 3: Determination of $(m_t/\Delta p)$ and $(b_t S_f/\Delta p)$

- Construct a plot Cartesian of $1/q$ vs. t^n.
- Fit a straight line through this data.
- Slope of this line gives the value of $(m_t/\Delta p)$ and $(b_t S_f/\Delta p)$ can be determined from the intercept of the line.

Step 4: Rate (q) and cumulative production (G_P) prediction

- If the $b_t S_f$ value calculated in the step 3 comes out to be zero, use the equation from table 6-3 to calculate the future rate and cumulative production.
- If the $b_t S_f$ value calculated in the step 3 comes out to be a non-zero number, use equations from table 6-5, 6-7, or 6-9 to calculate the future production and cumulative production depending on the value of n calculated in step 1.

6 Decline curve analysis of data generated using linear flow equation

6.1 Constant pressure drawdown

For constant pressure drawdown, the following reservoir properties listed in table 6-1 were considered for calculating the rate and cumulative production data.

Table 6-1: Reservoir properties considered for generation of flow rate and cumulative production using linear flow equation

Parameter	Value
Initial Reservoir Pressure (p_i)	4000 psi
Bottom hole pressure (p_{wf})	400 psi
Reservoir gas composition	100% CH_4
Critical temperature of CH_4 ($T_{C,CH4}$)	343 R
Critical pressure of CH_4 ($p_{C,CH4}$)	637 psi
Reservoir temperature (T_{res})	200 F
Formation thickness (h)	75 ft
Fracture half-length (L_f)	330 ft
Formation permeability (k)	0.0001 mD
Formation porosity (ϕ)	0.06
Initial gas saturation (S_g)	80%
Initial water saturation (S_w)	20%
Formation compressibility (C_f)	4×10^{-6} psi^{-1}
Width of fracture (w)	0.01 ft
Fracture permeability (k_f)	10000 mD

As the reservoir gas is assumed to be methane, the reduced temperature and pressure are given by:

$$T_R = \frac{T}{T_{C,CH_4}} = \frac{200+460}{343} = 1.92, \text{ and} \tag{97}$$

$$p_r = \frac{p}{p_{c,CH_4}} = \frac{4000}{637} = 5.94. \tag{98}$$

Using Standing and Katz gas deviation-factor chart (Katz, 1959) for natural gases, at initial reservoir conditions, $z = 0.98$.

The value of gas formation volume factor is given by:

$$B_g = \frac{5.03676ZT}{P}\ (RB/Mscf)\ . \tag{99}$$

Substituting the values of gas deviation-factor (z), temperature (T), and pressure (p) in the equation of 99, gas formation volume factor (B_g) can be calculated as follows:

$$B_{gi} = \frac{5.03676\times0.98\times(200+460)}{4000}\frac{RB}{Mscf} = 0.8144\ (RB/Mscf). \tag{100}$$

Using the Carr et al. (1954) viscosity nomograms, viscosity can be calculated as:

$$\mu = \frac{\mu}{\mu_1}\times\mu_1 = (0.0124\times1.51)cP = 0.0187\ cP. \tag{101}$$

Gas compressibility is calculated using equation 102,

$$c_g = \frac{1}{p_r p_{pc}} - \frac{1}{z}\left(\frac{\partial z}{\partial p_r}\right)_{T_r}, \tag{102}$$

where p_r is the reduced pressure, p_{pc} is the pseudocritical pressure of a gas mixture, z is the gas deviation factor, T_r is the reduced temperature. The value of $\left(\frac{\partial z}{\partial p_r}\right)_{T_r}$ was calculated from the slope of graph between p_r vs. z using the Standing and Katz gas deviation-factor chart (Katz, 1959) for the T_r and p_r calculated at the initial reservoir conditions. The value of gas compressibility was calculated to be $1.95\times10^{-4}\ psi^{-1}$.

Total formation compressibility is given by:

$$c_t = S_g c_g + S_w c_w + c_f, \tag{103}$$

where S_g is the saturation of gas, c_g is the compressibility of gas, S_w is the water saturation, c_w is the compressibility of water, c_f is the formation compressibility.

Using typical values of water and formation compressibility in equation 103, total formation compressibility can be calculated as:

$$c_t = \{(0.8\times0.000195) + (0.2\times3.6\times10^{-6}) + (4\times10^{-6})\}\ psi^{-1} = 1.61\times10^{-4}\ psi^{-1} \tag{104}$$

As given in tables 5-1, 5-2 and 5-4, flow rate (q), cumulative production (G_P), for linear flow condition are given by:

Table 6-2: Equations used to calculate the flow rate and cumulative production for the given reservoir

Parameter	**Linear flow ($S_f \neq 0$)**	**Linear flow ($S_f = 0$)**
m_t	$\frac{4.046B}{hL_f}\left(\frac{\mu}{k\phi c_t}\right)^{1/2}$	$\frac{4.046B}{hL_f}\left(\frac{\mu}{k\phi c_t}\right)^{1/2}$
b_t	$\frac{141.2qB\mu}{kh}$	$\frac{141.2qB\mu}{kh}$

Table 6-2 continued		
Parameter	**Linear flow ($S_f \neq 0$)**	**Linear flow ($S_f = 0$)**
q	$\frac{\Delta p}{m_t t^{1/2} + bS_f}$	$\frac{\Delta p}{m_t t^{1/2}}$
G_P	$\frac{2\Delta p}{m_t}\left\{t^{0.5} - cln\left(\frac{t^{0.5}}{c} + 1\right)\right\}$	$\frac{2\Delta p t^{1/2}}{m_t}$

Flow rate and cumulative production data was calculated for two cases under constant pressure drawdown, first when fracture skin is zero and second when fracture skin is 0.1. The original Duong method and the modified Duong method were then applied to 6 months of data to calculate the respective model parameters using which rate and cumulative production forecasts were generated for 2 years. The predicted results were then compared to the actual data generated using linear flow equation given by equation 50.

Three cases considered for analysis under constant pressure condition are:

Case 1: Constant pressure drawdown, linear flow $S_f = 0$ and Δp data is available,

Case 2: Constant pressure drawdown, linear flow $S_f = 0.1$ and Δp data is available, and Case 3: Constant pressure drawdown, linear flow $S_f = 0.1$ and Δp data is not available.

6.1.1 Case 1: Linear flow $S_f = 0$ and Δp data available

Duong method

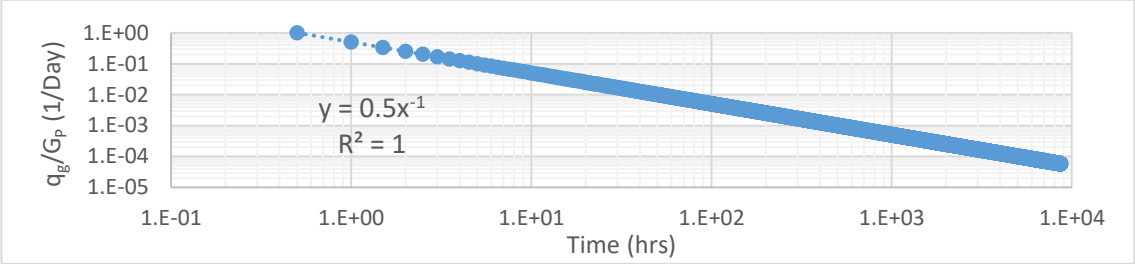

Figure 6.1: Step 2 of Duong's method, calculation of 'a' and 'm'

In this case, $a = (1 - n) = 0.5$ and $m = 1$. This result is in accordance with our theory that Duong model will follow the rigorous mathematical expression of $\frac{q}{G_P} = \frac{1-n}{t}$ for constant bottomhole pressure and zero fracture skin conditions.

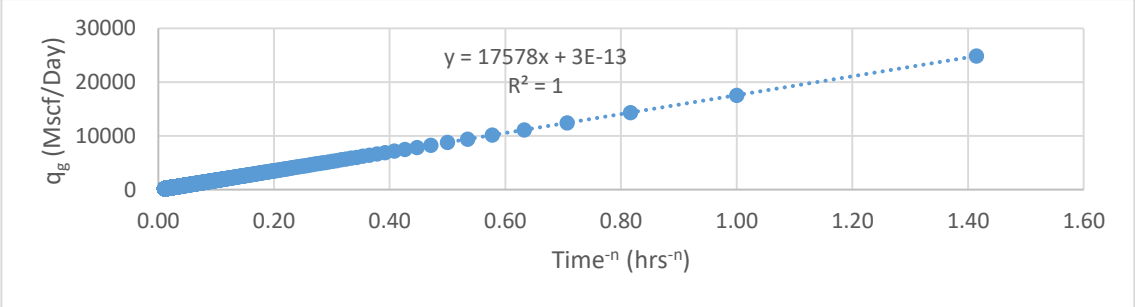

Figure 6.2: Step 3 of Duong method, calculation of q_1

As $m = 1$ in this case, q_1 has to be calculated from the slope of a graph between q_g and t^{-n} as it can be seen from equation 12.

Table 6-3: Parameters obtained for Duong Model, case 1

Duong's Model parameters	Actual Value	Calculated Value
a	0.5	0.5
m	1	1
q_1 (Mscf/Day)	17578.05	17578

Modified Duong Method

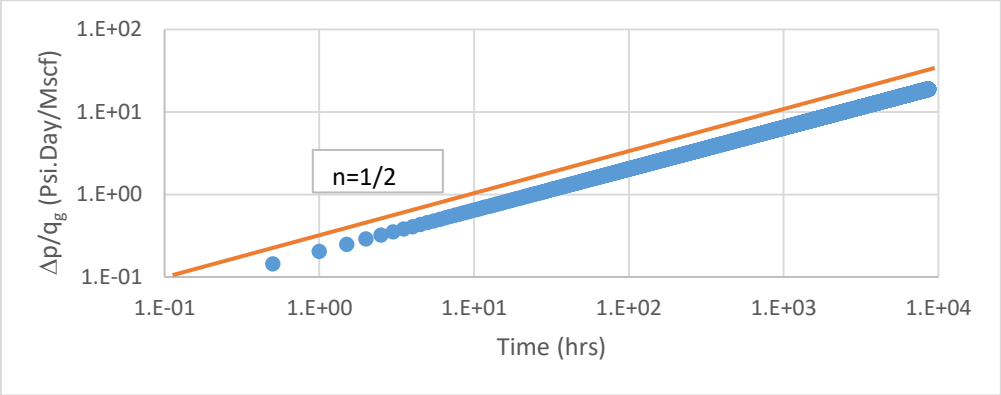

Figure 6.3: Step 2 of Modified Duong method: Determination of 'n'

Due to zero fracture skin, we see $n = 1/2$ from $t = 0$ hrs.

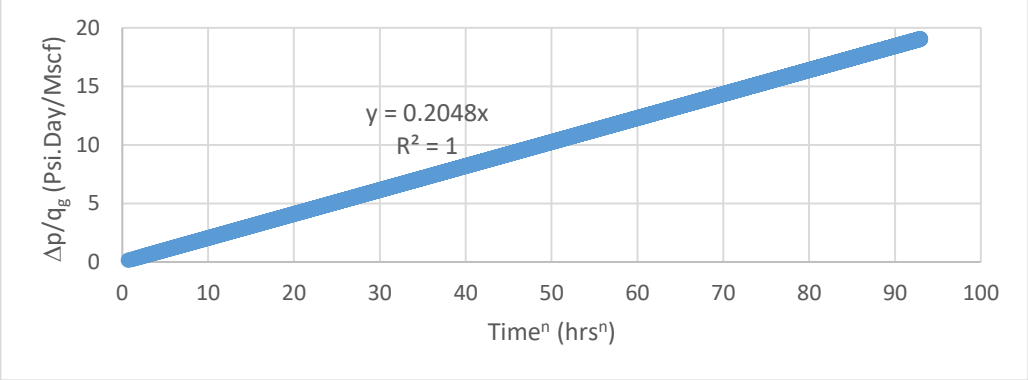

Figure 6.4: Step 3 of Modified Duong method, Determination of 'm_t' and 'b_tSf'

The straight line fitted between $\Delta p/q_g$ and t^n passes through origin because we have zero fracture skin in the system.

Table 6-4: Parameters obtained for modified Duong model, case 1

Modified Duong's Model parameters	Actual Value	Calculated Value
n	1/2	1/2
m_t	0.2048	0.2048
b_tS_f	0	0

Comparison of prediction results

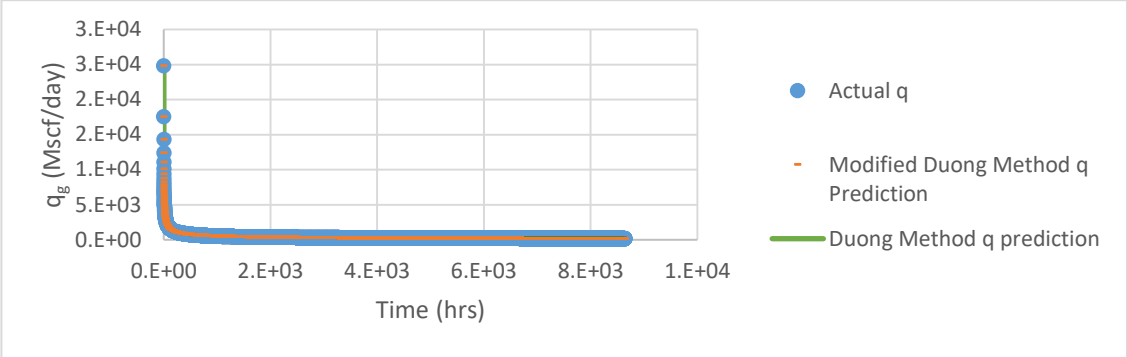

Figure 6.5: Flow rate prediction comparison

Perfect rate match is obtained by using Duong method and Modified Duong method as we have a constant bottomhole production with zero fracture skin. These conditions meet the requirements for which the Duong method and the limiting case of Modified Duong method have been derived.

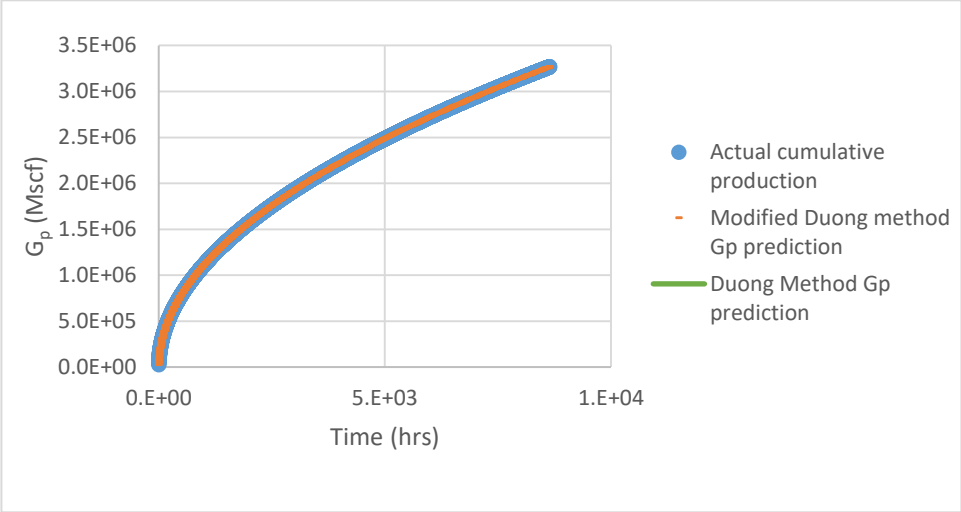

Figure 6.6: Cumulative production prediction comparison

Perfect cumulative production match obtained by using Duong method and Modified Duong method as we have a constant bottomhole production with zero fracture skin which satisfy the conditions based on which both the methods have been derived.

6.1.2 Case 2: Linear flow $S_f = 0.1$ and Δp data available

Duong method

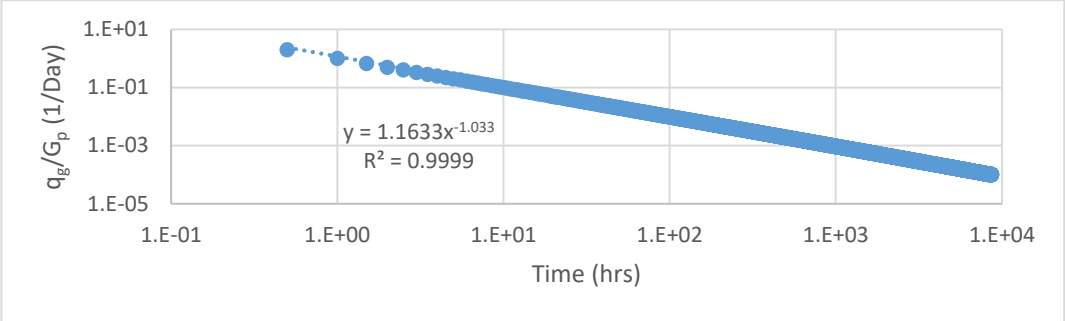

Figure 6.7: Step 2 of Duong method, determination of 'a' and 'm'

Due to presence of fracture skin, the value of m is no longer 1. Here, the value of m is 1.1633 which is greater than 1.

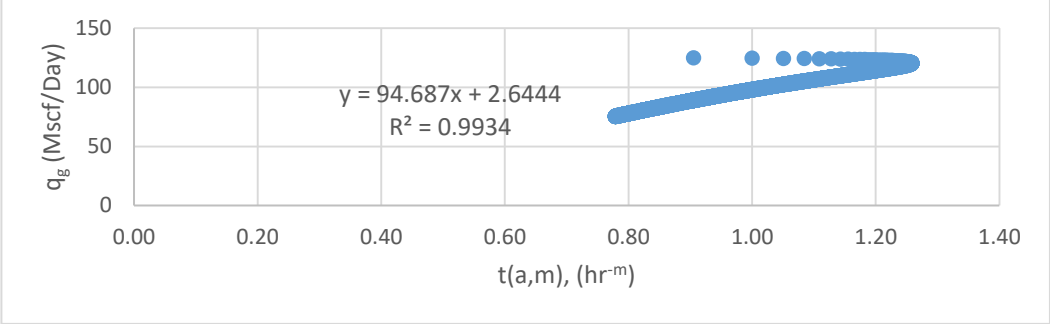

Figure 6.8: Step 3 of Duong method, determination of 'q_1'

$t(a,m)$ shows non-monotonic behavior. This leads to some error in calculation of q_1 when trying to fit a linear trendline through the plotted data.

Table 6-5: Parameters obtained for Duong method, case 2

Duong's Model parameters	Actual Value	Calculated Value
a	-	1.1633
m	-	1.033
q_1 (Mscf/Day)	124.67	94.69

Modified Duong Method

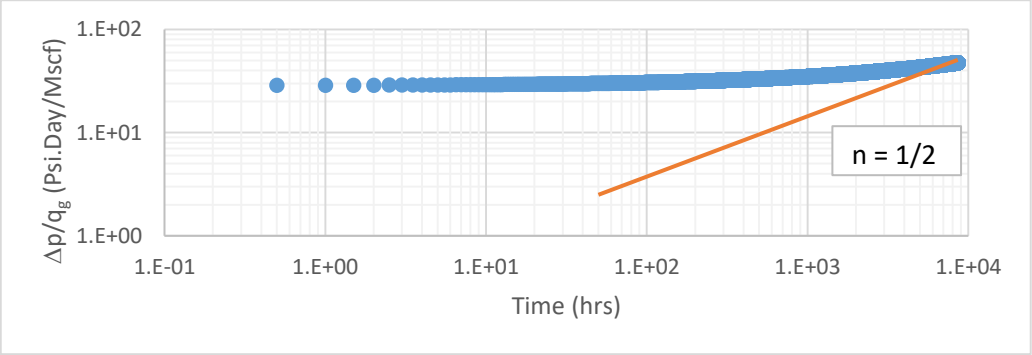

Figure 6.9: Step 2 of modified Duong model, determination of 'n'

The value of n is masked due to to presence of fracture skin. As suggested in the workflow, it is best to use pressure derivative to calculate the value of n, since the pressure derivative remains unaffected from presence of fracture skin.

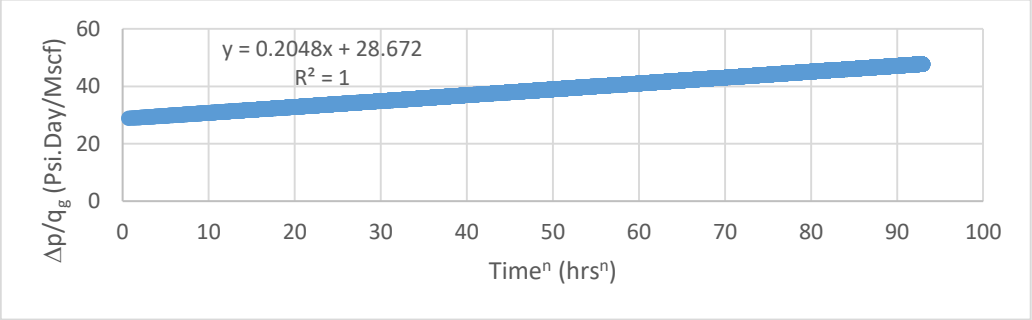

Figure 6.10: Step 3 of Modified Duong method, Determination of 'm_t' and 'b_tSf'

Table 6-6Parameters for Modified Duong model, case 2

Modified Duong's Model parameters	Actual Value	Calculated Value
n	1/2	n value masked due to fracture skin
m_t	02048	0.2048
b_tS_f	28.672	28.672

Comparison of prediction result

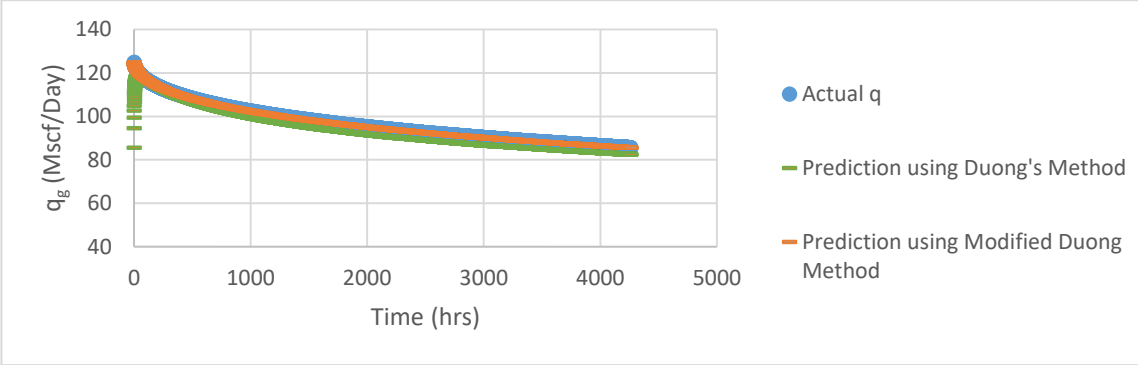

Figure 6.11: Flow rate prediction comparison

Modified Duong method flow rate prediction matches perfectly with the actual flow rate while Duong Method underestimates the flow rate. It should be noted that the flow rate prediction from Modified Duong Method is non-monotonic in nature due to non-monotonic $t(a, m)$. Flow rate increases initially, and then starts decreasing.

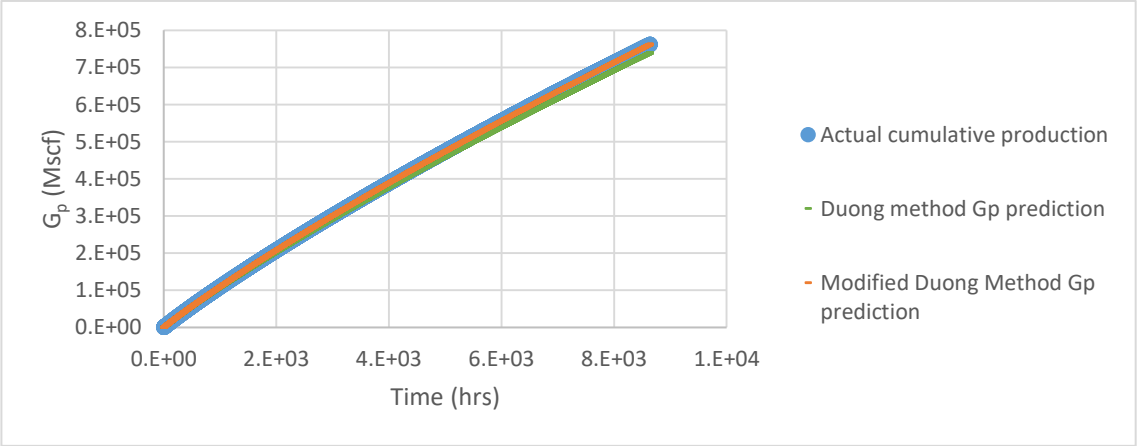

Figure 6.12: Cumulative production prediction comparison

Modified Duong method gives a perfect match with the actual cumulative production. Duong method underestimates the cumulative production.

6.1.3 Case 3: Linear flow, $S_f = 0.1$ and Δp value is not available

Duong Method

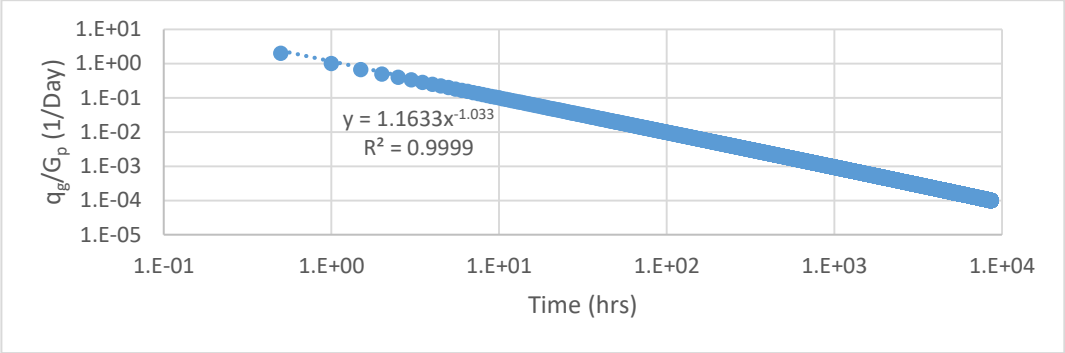

Figure 6.13: Step 2 of Duong method, determination of 'a' and 'm'

Under constant pressure condition, there is no change in the Duong method results in absence of pressure data.

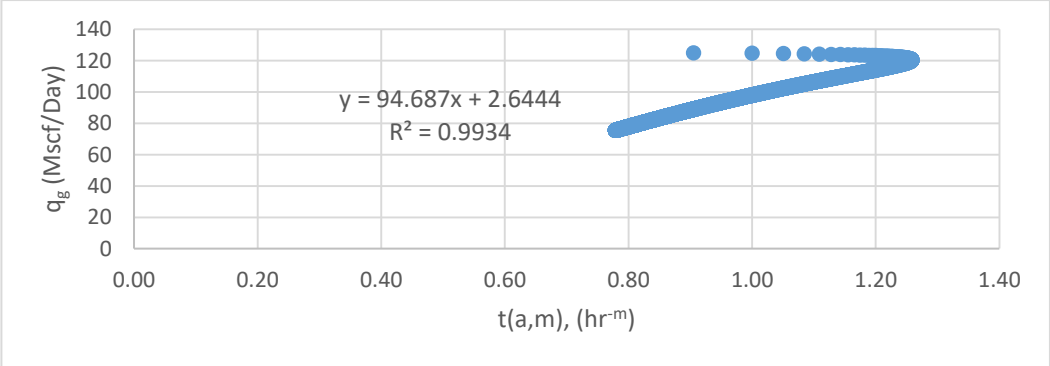

Figure 6.14: Step 3 of Duong method, determination of 'q_1'

Non-monotonicity in $t(a, m)$ can be observed here.

Table 6-7: Parameters obtained for Duong method, case 3

Duong's Model parameters	Actual Value	Calculated Value
a	-	1.1633
m	-	1.033
q_1 (Mscf/Day)	124.67	94.69

Modified Duong Method

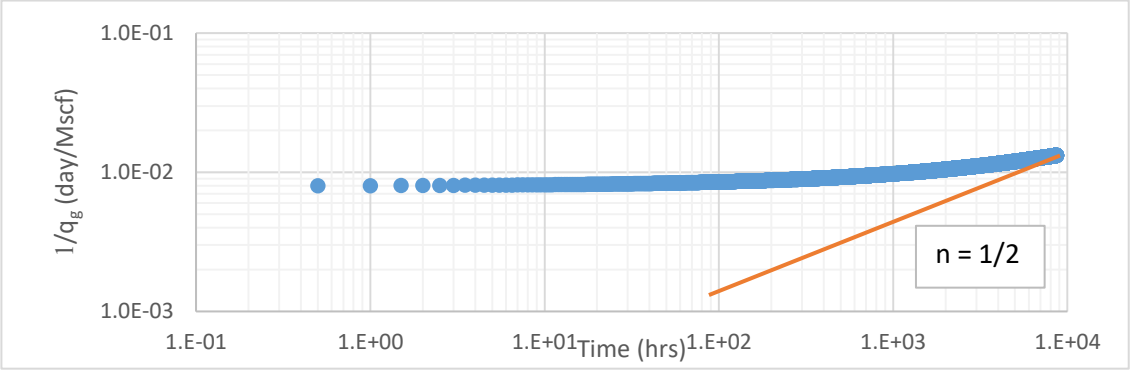

Figure 6.15: Step 2 of Modified Duong method (determination of 'n') in absence of Δp values

The actual value of n has been masked due to presence of fracture skin.

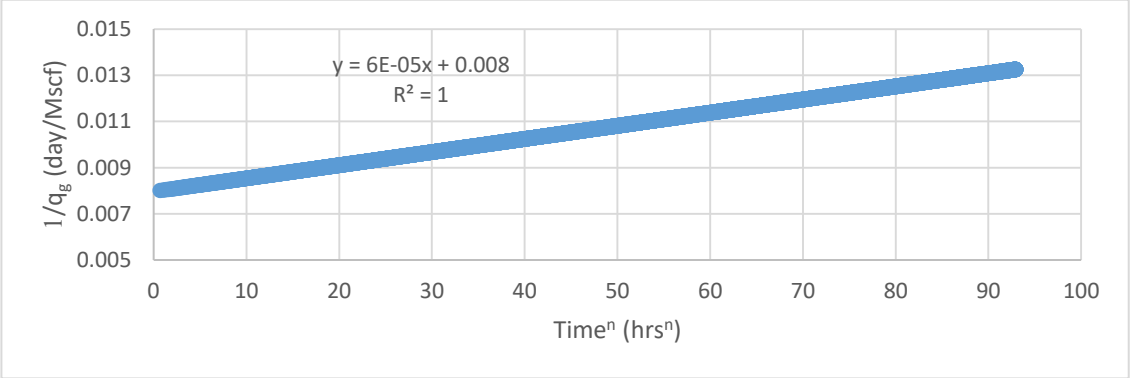

Figure 6.16: Step 3 of Modified Duong method (determination of $m_t/\Delta p$ and $b_tS_f/\Delta p$) in absence of Δp value

Table 6-8: Parameters obtained for modified Duong method, case 3

Modified Duong's Model parameters	Actual Value	Calculated Value
n	1/2	n value masked due to fracture skin
$m_t/\Delta p$	5.6×10^{-5}	6×10^{-5}
$b_tS_f/\Delta p$	0.008	0.008

Comparison of prediction result

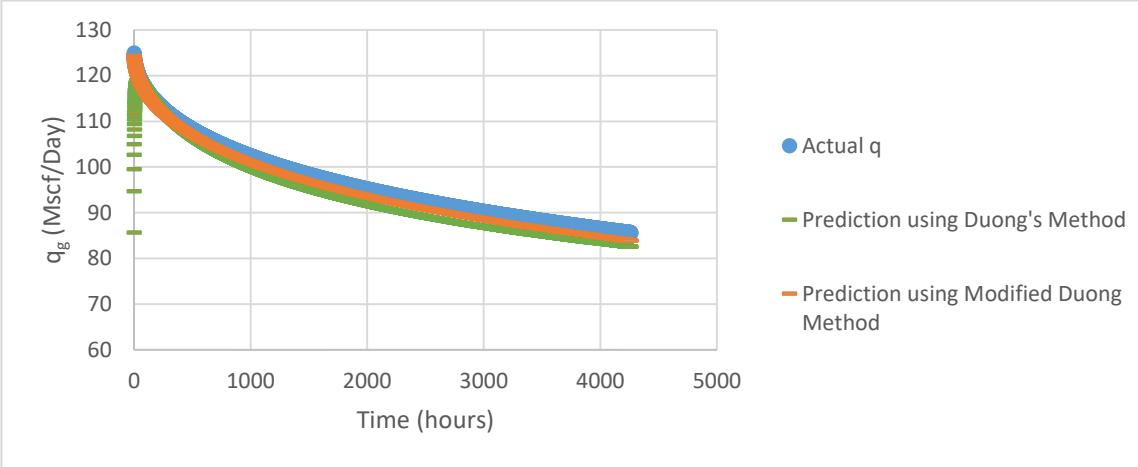

Figure 6.17: Flow rate prediction comparison

Under constant pressure, modified Duong method works perfectly and gives a good match for flow rate prediction and Duong method is underestimating the flow rate, same as in case 2.

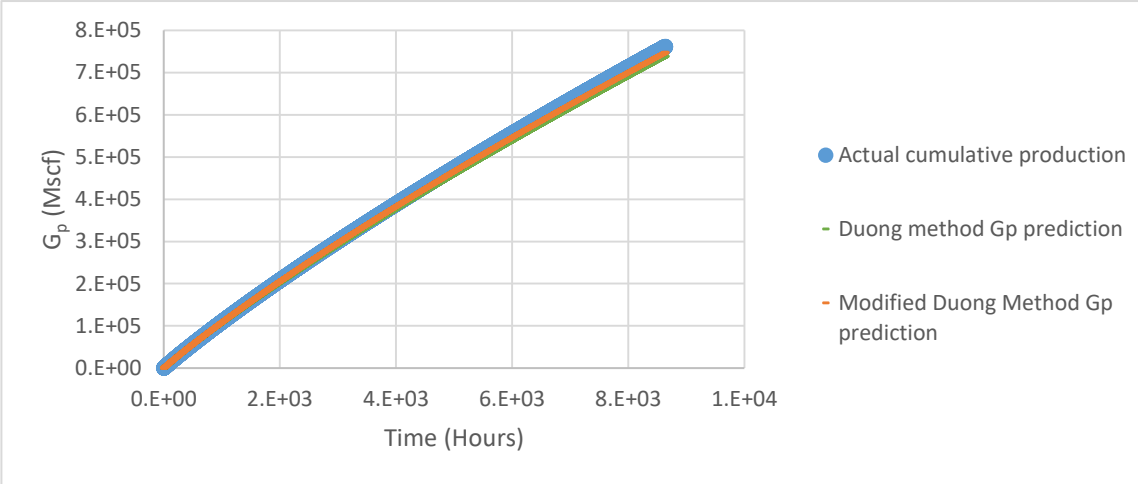

Figure 6.18: Cumulative production prediction comparison

Under constant pressure, modified Duong method gives a perfect match with the cumulative production and Duong method prediction is underestimating the cumulative production.

6.2 Variable pressure drawdown

Under variable pressure conditions, we expect a poor performance from Duong method as the equations derived in the Duong method are conditioned on a constant pressure production. Modified Duong method is expected to do fairly well due to use of normalized pressure in determination of n, m_t and $b_t\, S_f$. Use of normalized pressure negates the effect of changing bottomhole pressure and helps us obtain better results. However, in absence of pressure data, Modified Duong method is also subjected to errors, similar to the Duong method.

For decline curve analysis in variable pressure drawdown analysis, reservoir properties are kept same as that of section 6.1 and bottomhole pressure is decreased linearly from 1800 psi to 400 psi over a time interval of 6 months.

One year of flow rate and cumulative production data is used to calculate Duong and Modified Duong model parameters. Using these parameters, forecast for three years are made for following three cases:

Case 4: Variable pressure drawdown, linear flow $S_f = 0$ and Δp data is available,

Case 5: Variable pressure drawdown, linear flow $S_f = 0.1$ and Δp data is available, and Case 6: Variable pressure drawdown, linear flow $S_f = 0.1$ and Δp data is not available.

6.2.1 Case 4: Linear flow $S_f = 0$ and Δp data available

Duong Method

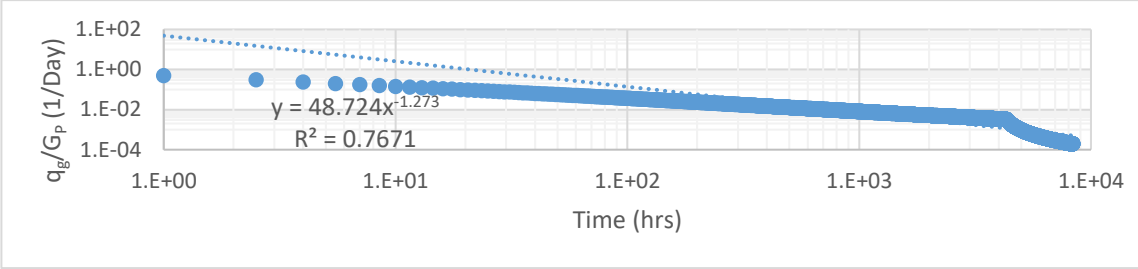

Figure 6.19: Step 2 of Duong method, determination of 'a' and 'm'

We can notice the sharp inflection point when the production shifts from varying bottomhole pressure to constant bottomhole pressure condition. This change in slope leads to wrong calculation of Duong's model parameter (a and m).

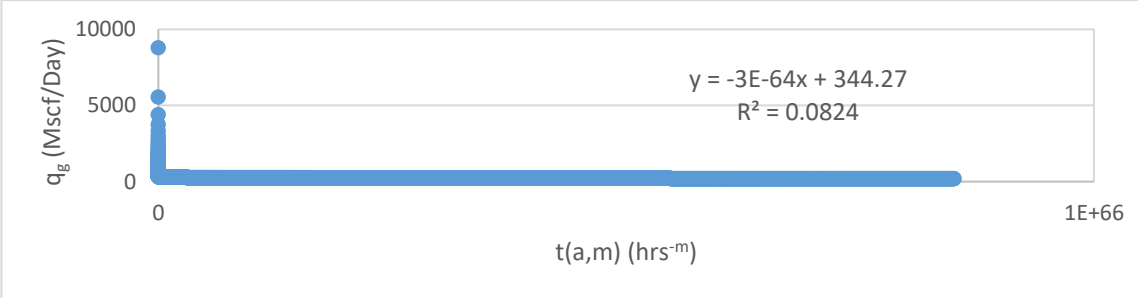

Figure 6.20 Step 3 of Duong method, q_1 calculation

For variable pressure, $t(a, m)$ does not behave monotonically and we end up getting a negative value for q_1.

Table 6-9: Parameters obtained for Duong model, case 4

Duong's Model parameters	Expected Value	Calculated Value
a	-	48.724
m	-	1.273
q_1 (Mscf/Day)	-	-1×10^{-64}

Modified Duong Model

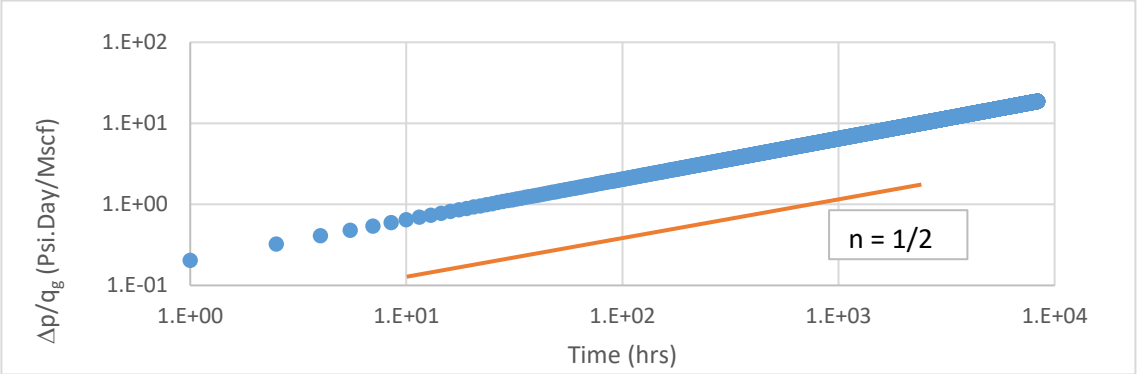

Figure 6.21: Step 2 of Modified Duong Model, determination of n

Use of normalized pressure negates the effect of changing bottomhole pressure. As we have zero facture skin in the system, we see $n = 1/2$ in the system from $t = 0$.

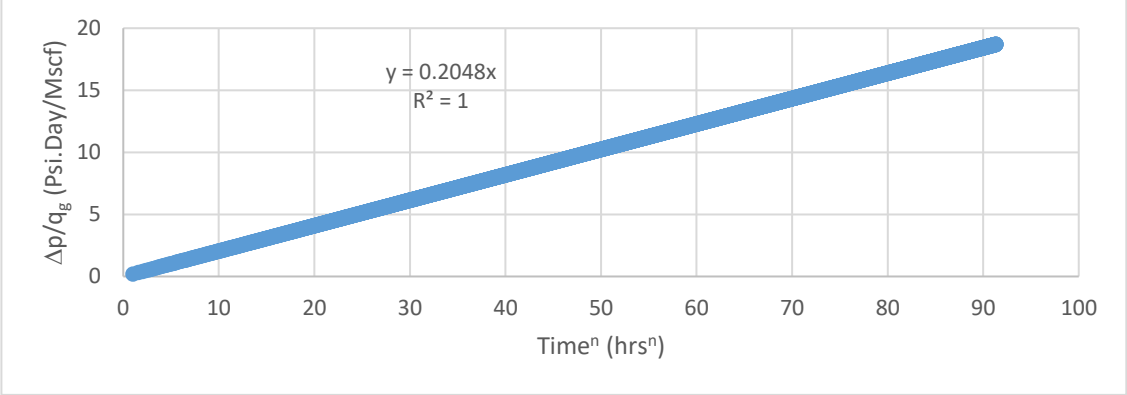

Figure 6.22: Step 3 of Modified Duong Method, determination of 'm_t' and 'b_tS_f'

Table 6-10: Parameters obtained for modified Duong method, case 4

Modified Duong's model parameters	Actual Value	Calculated Value
n	1/2	1/2
m_t	0.2048	0.2048
b_tS_f	0.00	0.00

Comparison of prediction results

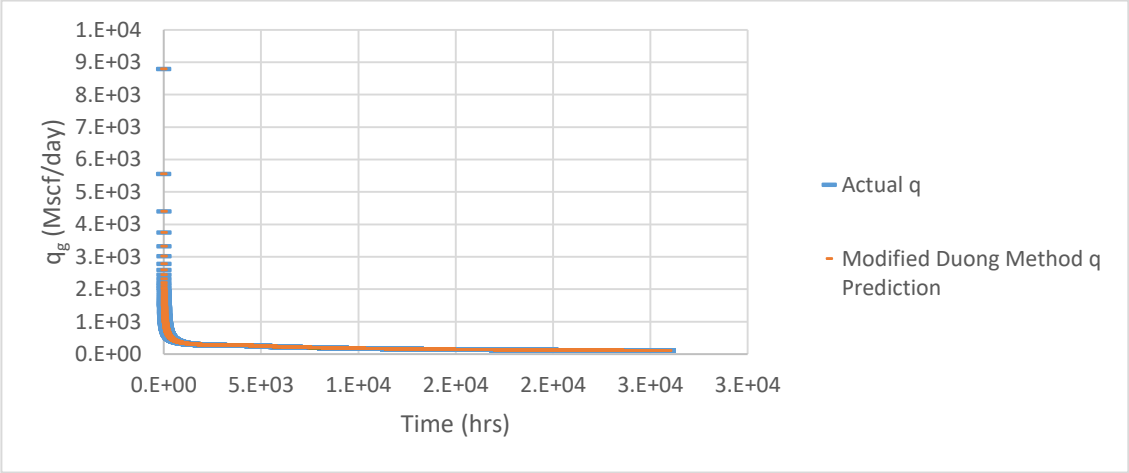

Figure 6.23: Flow rate prediction comparison

Modified Duong method gives a perfect rate prediction for varying bottomhole pressure while Duong method fails to make any predictions due to negative values of q_1.

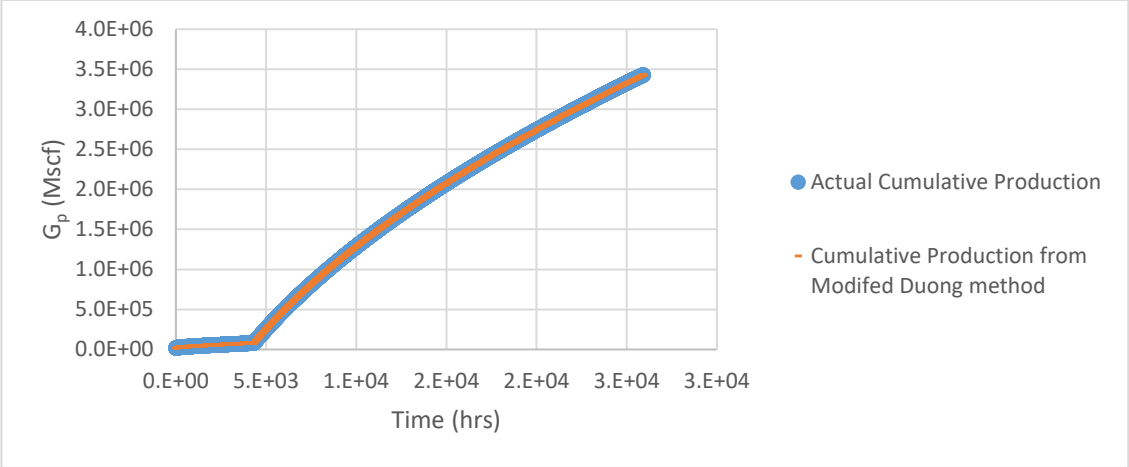

Figure 6.24: Cumulative production prediction comparison

Modified Duong method gives a good cumulative production prediction for varying bottomhole pressure while Duong method fails to provide any prediction due to negative value of q_1.

6.2.2 Case 5: Linear flow $S_f = 0.1$ and Δp data available

Duong method

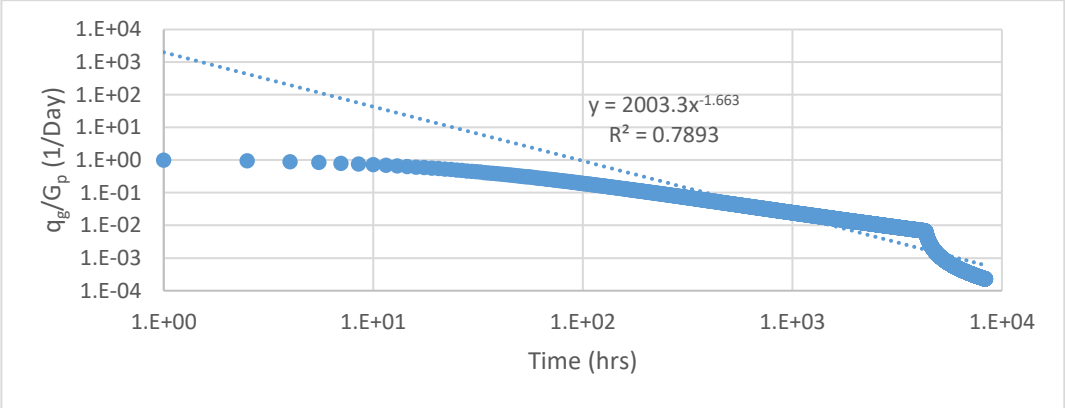

Figure 6.25: Step 2 of Duong's method, determination of 'a' and 'm'

Due to changing bottomhole pressure, the graph shows an inflection point at the time when we switch from varying bottomhole pressure to constant bottomhole pressure production. This leads to errors in determination of a and m when trying to fit a straight line through the data with changing slopes.

The values of a and m obtained for the variable bottom-hole pressure case with fracture skin are such that it is not possible to compute $t(a,m)$ for each time step. Therefore, q_1 cannot be calculated in this case.

Table 6-11: Parameters obtained for Duong method, case 5

Duong's Model parameters	Expected Value	Calculated Value
a	-	2003.3
m	-	1.663
q_1 (Mscf/Day)	-	Not possible to calculate

Modified Duong method

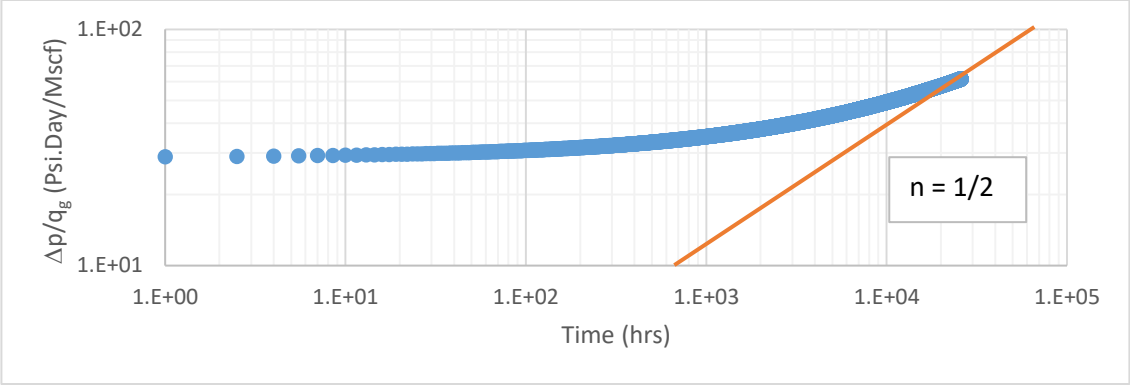

Figure 6.26: Step 2 of modified Duong method, determination of 'n'

Initial value of n is masked due to presence of fracture skin in the system. After sufficient time, when $m_t t^n$ become significantly larger than $b_t S_f$, we can see the correct value of n.

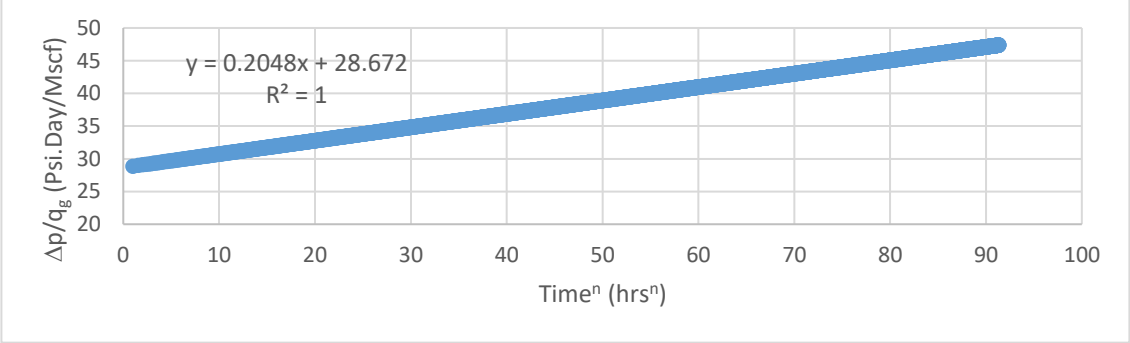

Figure 6.27: Step 2 of modified Duong method, determination of 'm_t' and '$b_t S_f$'

Use of normalized pressure negates the effect of changing bottomhole pressure.

Table 6-12: Parameters obtained for modified Duong model, case 5

Modified Duong's model parameters	Actual Value	Calculated Value
n	1/2	n *value masked due to fracture skin*
m_t	0.2048	0.2048
$b_t S_f$	28.672	28.672

Comparison of prediction results

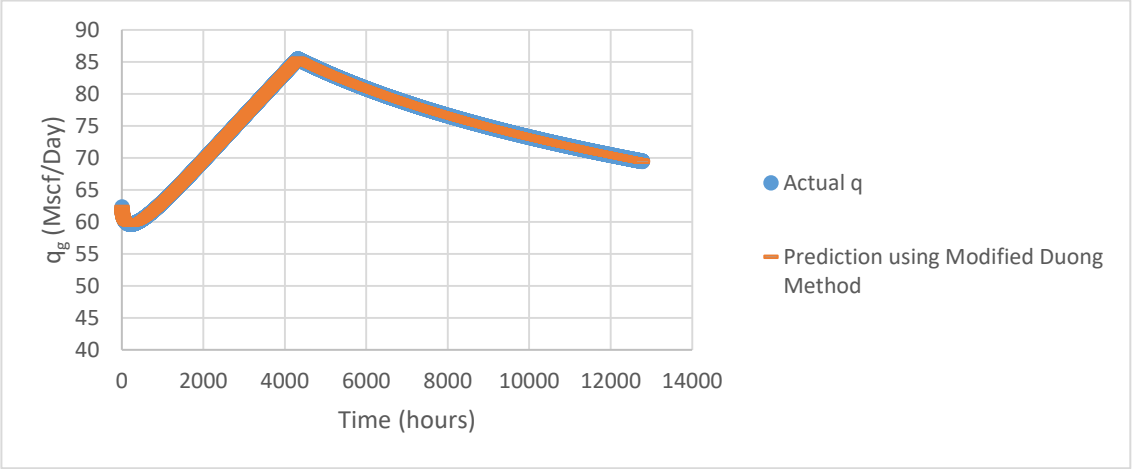

Figure 6.28: Flow rate prediction comparison

Very good rate prediction is observed by using Modified Duong method. Modified Duong method fails to make any predictions as we cannot calculate the value of $t(a, m)$.

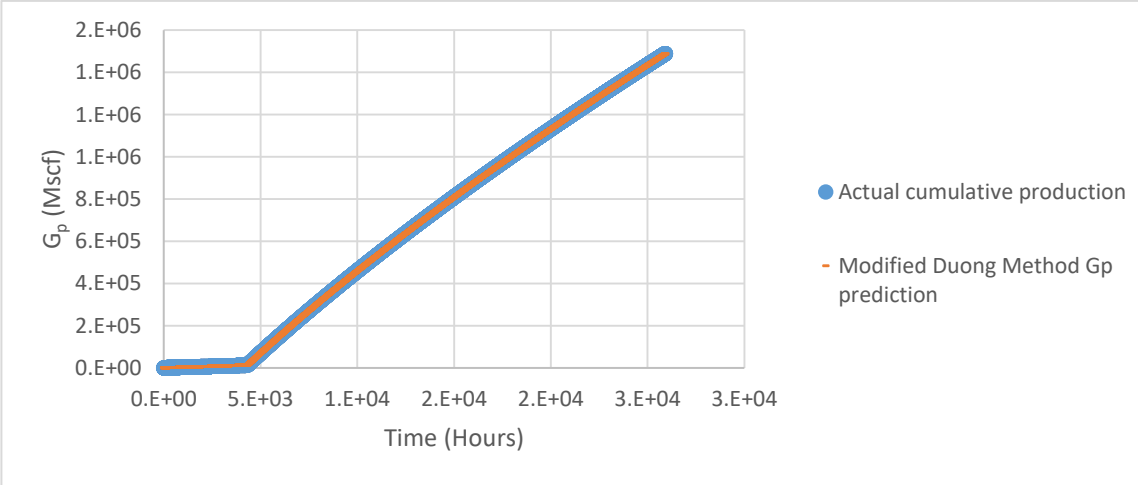

Figure 6.29: Cumulative production prediction comparison

Very good cumulative production prediction match is obtained using Modified Duong method.

6.2.3 Case 6: Linear flow $S_f = 0.1$ and Δp value not available

The availability of pressure data in this case for Duong method is not going to make any difference. Therefore, our results remain same as that of case 5 analyzed for Duong method.

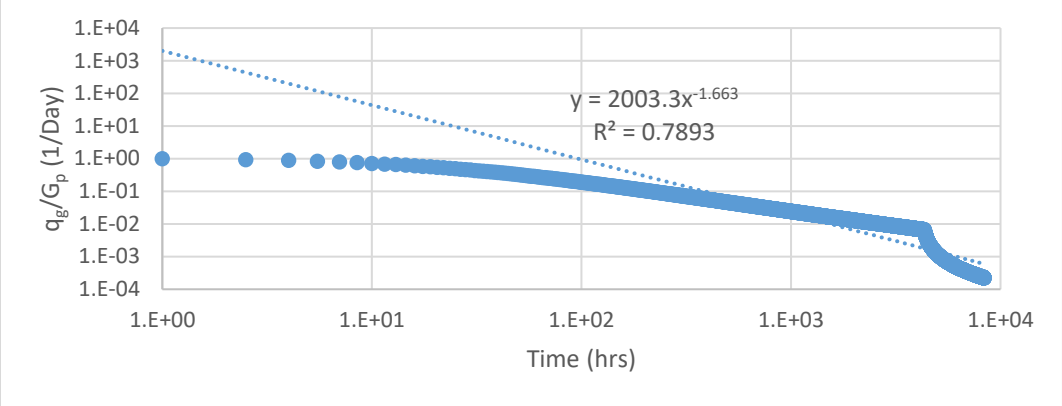

Figure 6.30: Step 2 of Duong's method, determination of 'a' and 'm'

Due to changing bottomhole pressure, the graph shows an inflection point at the time when we switch from varying bottomhole pressure to constant bottomhole pressure. This leads to errors in determination of a and m when trying to fit a straight line through the data with changing slopes.

As stated earlier, it is not possible to calculate q_1 in this case as we cannot compute $t(a, m)$ for the computed value of a and m.

Table 6-13: Parameters obtained for Duong model, case 6

Duong's Model parameters	Expected Value	Calculated Value
a	-	2003.3
m	-	1.663
q_1 (Mscf/Day)	-	Not possible to calculate

Modified Duong method

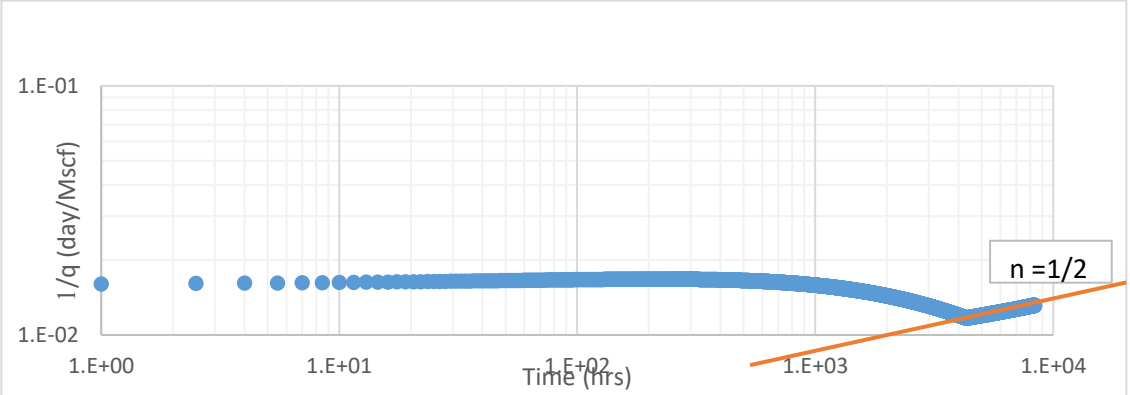

Figure 6.31: Step 2 of modified Duong method, determination of n

In the absence of pressure data, the graph between $1/q$ and $time$ gets affected by the pressure changes. Also, the presence of fracture skin masks the actual value of n until late time period.

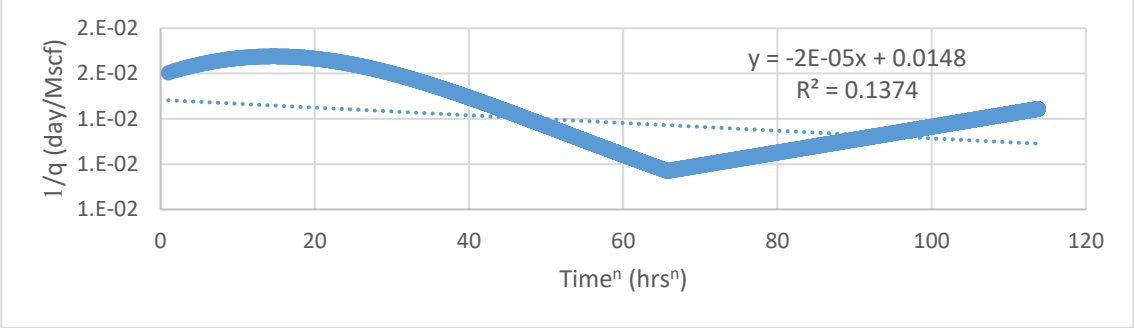

Figure 6.32: Step 3 of modified Duong method, determination of '$m_t/\Delta p$' and '$b_t S_f/\Delta p$'

In absence of pressure data for varying bottomhole pressure case, modified Duong method also starts facing issues as seen in the graph. Changes in bottomhole pressure leads to formation of spikes and drops in the data making it non-linear. Our attempts to fit a straight line through this non-linear section of data introduced errors in calculation of m_t and $b_t S_f$ as seen in graph 6.34.

As the value of m_t comes out to be negative in this case, flow rate and cumulative production predictions cannot be made.

7 Decline curve analysis of simulated data

Reservoir properties are kept same as that of chapter 6 to model flow through a hydraulically fractured well using IHS software harmony. Fracture spacing is kept as 400ft. in the model. To reduce the computation time, flow to only one fracture is considered. Rate, pressure and cumulative production data are generated for 30 years under various specified conditions.

Using depth of investigation equation, the time to reach 200 ft. (half of fracture spacing length) comes out to be 1000 days.

7.1 Effect of wellbore storage

Wellbore storage masks and distorts the reservoir effects making it very difficult to get the correct flow rate for a given bottomhole pressure. This effect can last until pressure is equalized between the wellbore and the formation. The duration of wellbore primarily depends on three factors: the wellbore volume, the formation permeability, and the fluid compressibility. Large volumes, and lower permeability values can cause significant duration of wellbore storage in hydraulically-fractured low permeability horizontal well that could last months.

For comparing the prediction results between Duong method and Modified Duong method, we have considered cases where model parameters were tried to be calculated using 6 months of historical data. We understand that the wellbore storage may mask 6 months' initial production period data rendering this data unsuitable for the decline curve analysis purposes.

The time duration of data considered for our purposes is only for academic purposes and is not recommended for the real-life decline curve analysis.

7.2 Constant pressure drawdown

Determination of linear flow period by analyzing the $S_f = 0$ case

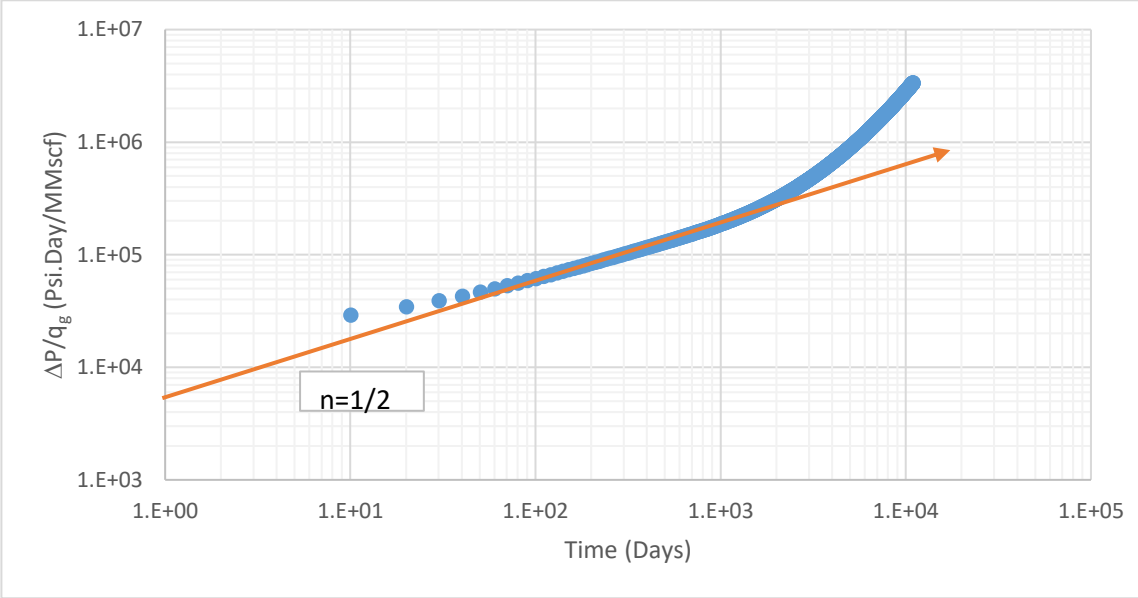

Figure 7.1: Determination of 'n' using zero fracture skin data

By comparing the graph data with $n = 1/2$ line, linear flow region can be seen between 50 day to 1000 days.

7.2.1 Case 1: Linear flow, $S_f = 0$ and Δp value available

Duong method using 6 months of data

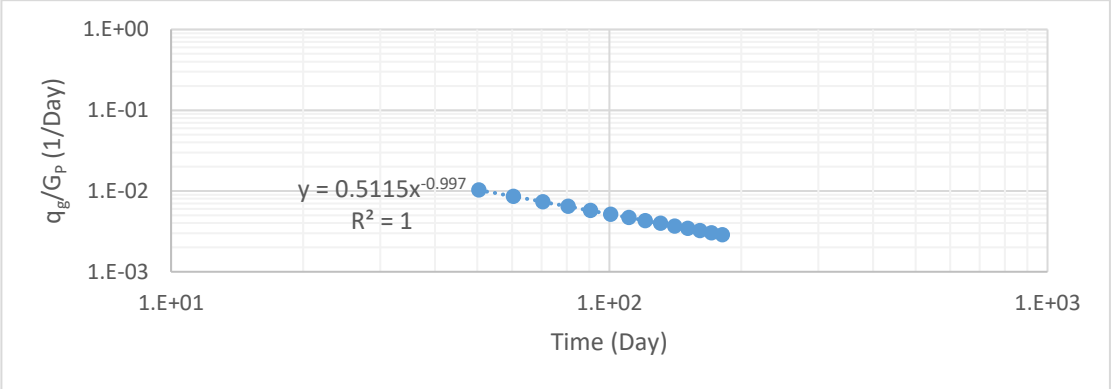

Figure 7.2: Step 2 of Duong method, determination of 'a' and 'm'

We observe a very good linear fit for the data in both the graphs for this case.

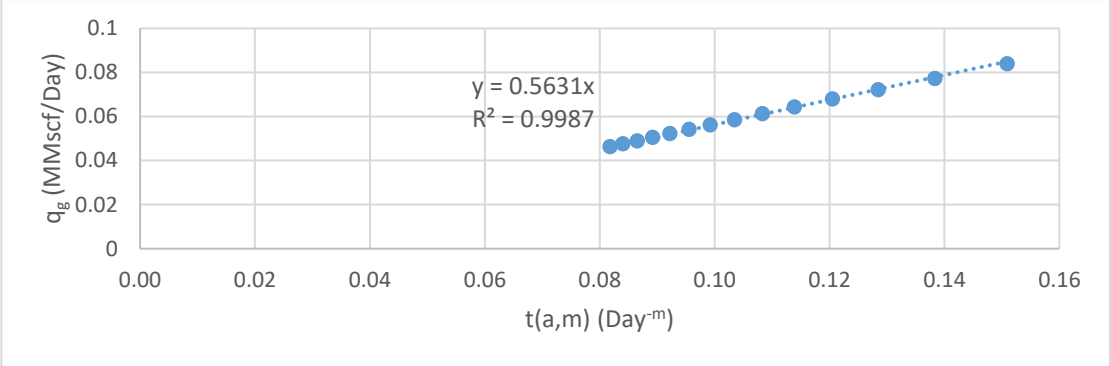

Figure 7.3: Step 3 of Duong method, determination of q_1

Table 7-1: Parameters obtained for Duong model, case 1

Duong's Model parameters	Calculated Value
a	0.5115
m	0.997
q_1 (MMscf/Day)	0.5631

Modified Duong method using 6 months of data

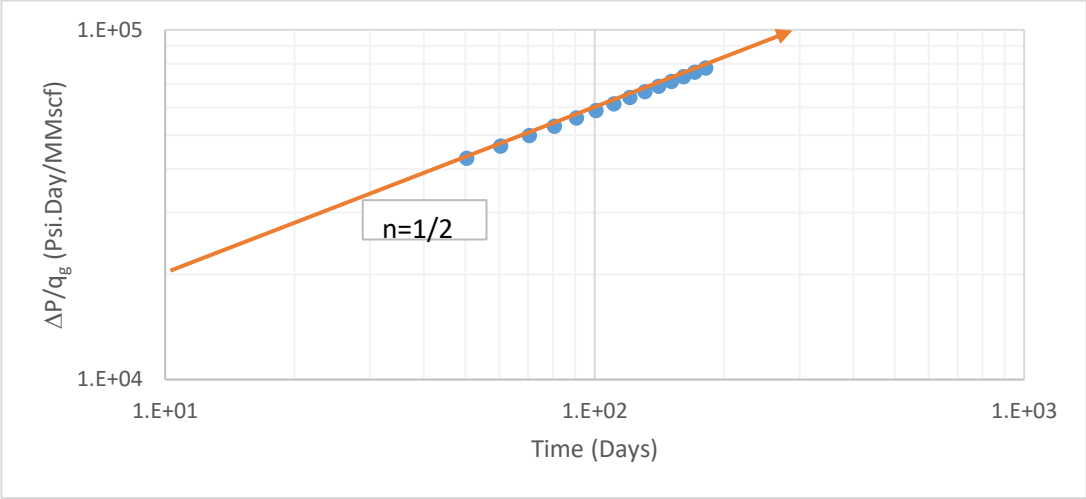

Figure 7.4: Step 2 of modified Duong model, determination of 'n'

We can observe a half slope from the very early on in the data as there is no fracture skin present in the system.

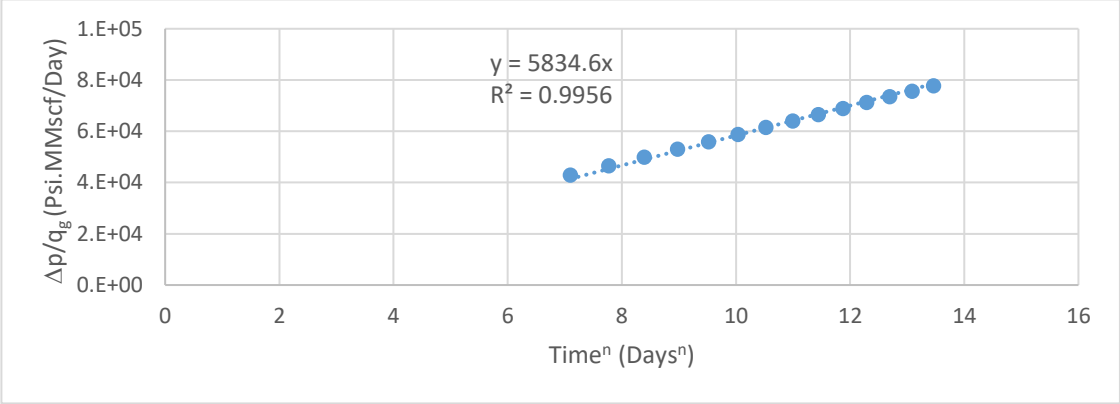

Figure 7.5: Step 3 of modified Duong model, determination of 'm_t' and 'b_tS_f'

Table 7-2: Parameters obtained for modified Duong model, case 1

Modified Duong's Model parameters	Calculated Value
n	1/2
m_t	5835.6
b_tS_f	0

Comparison of Prediction Results

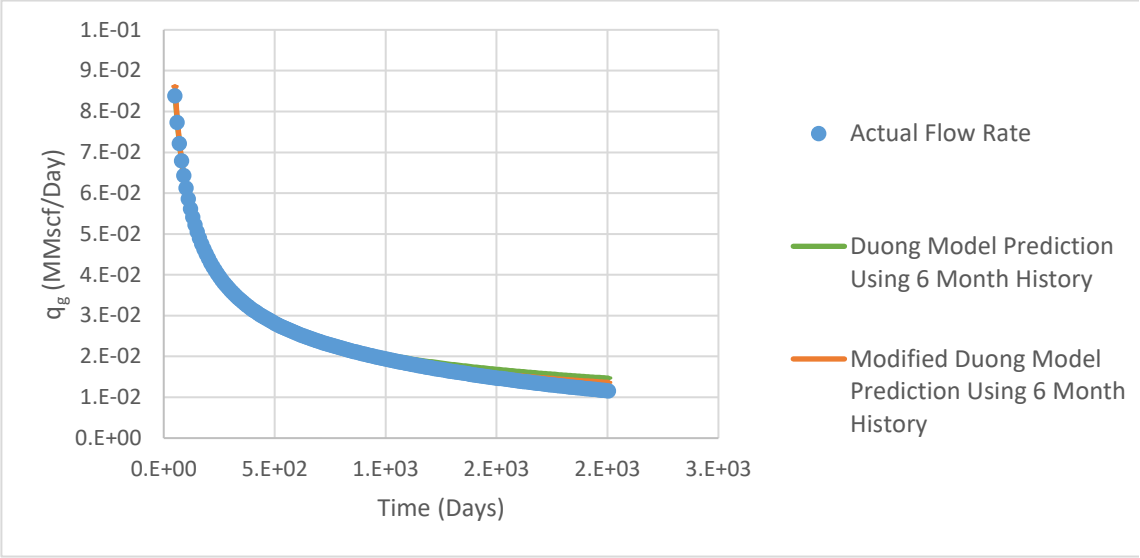

Figure 7.6: Flow rate prediction comparison

We obtain very good prediction matches for flow rate and cumulative production using both the methods with just 6 months of historical data.

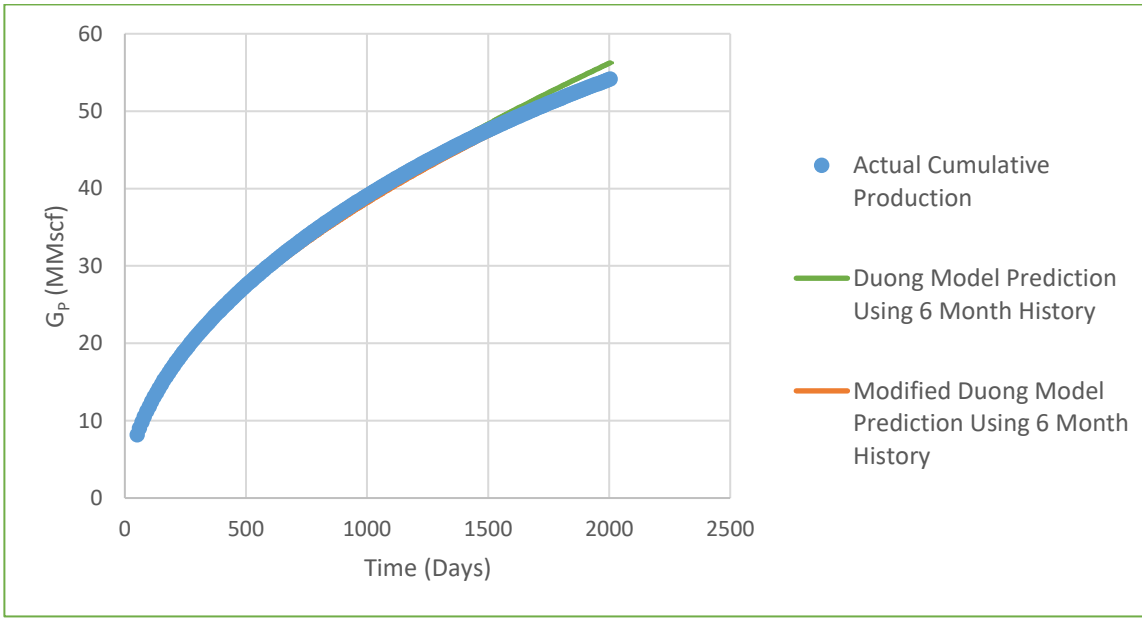

Figure 7.7: Cumulative production prediction comparison

7.2.2 Case 2: Linear flow, $S_f = 0.5$ and Δp value available

Duong method using 6 months of data

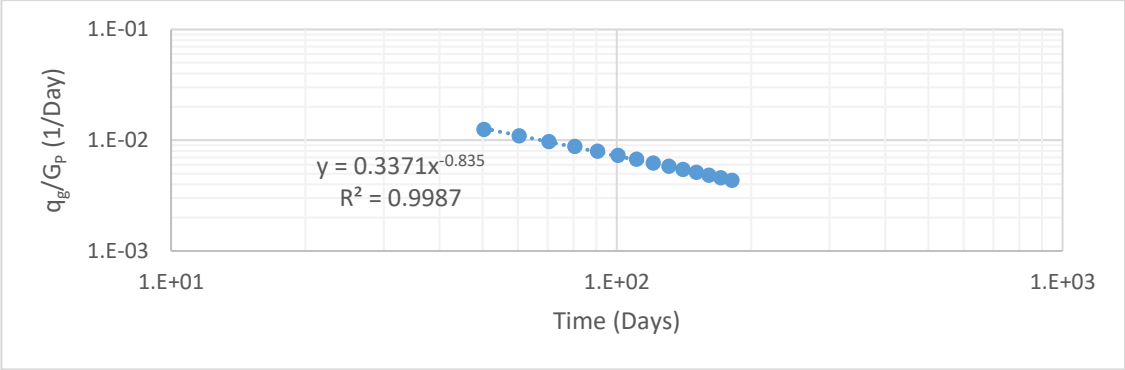

Figure 7.8: Step 2 of Duong method, determination of 'a' and 'm'

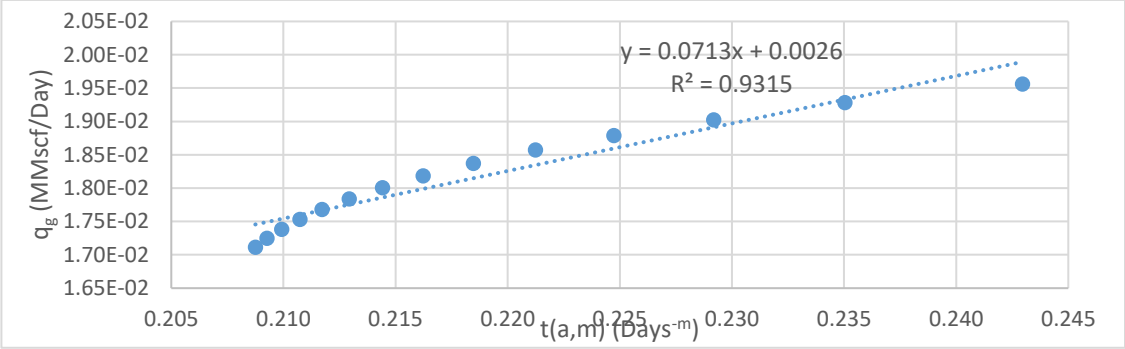

Figure 7.9: Step 3 of Duong method, determination of q_1

As it be seen in this case, introduction of fracture skin causes the a and m values to change. Also, the graph between q_g and $t(a,m)$ is not linear any more.

Table 7-3: Parameters obtained for Duong model, case 2

Duong's Model parameters	Calculated Value
a	0.3371
m	0.8350
q_1 (MMscf/Day)	0.0713

Duong method using 2 years of data

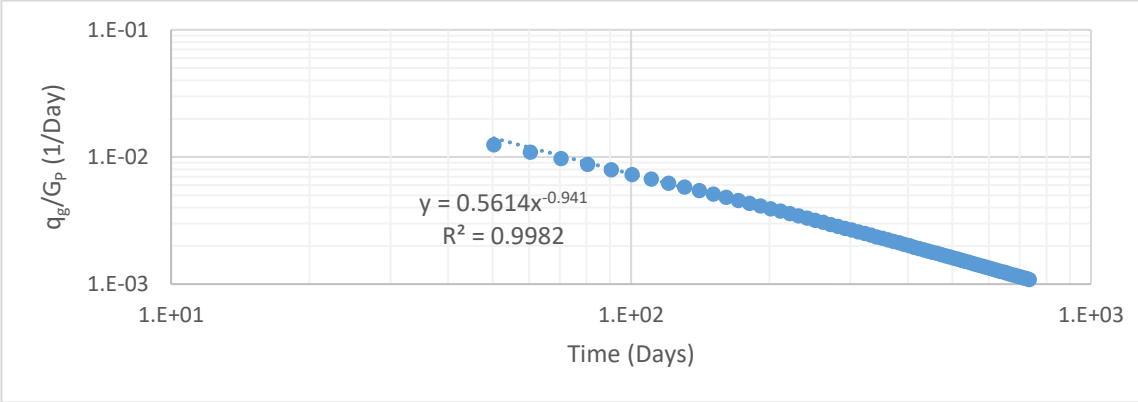

Figure 7.10: Step 2 of Duong method, determination of 'a' and 'm'

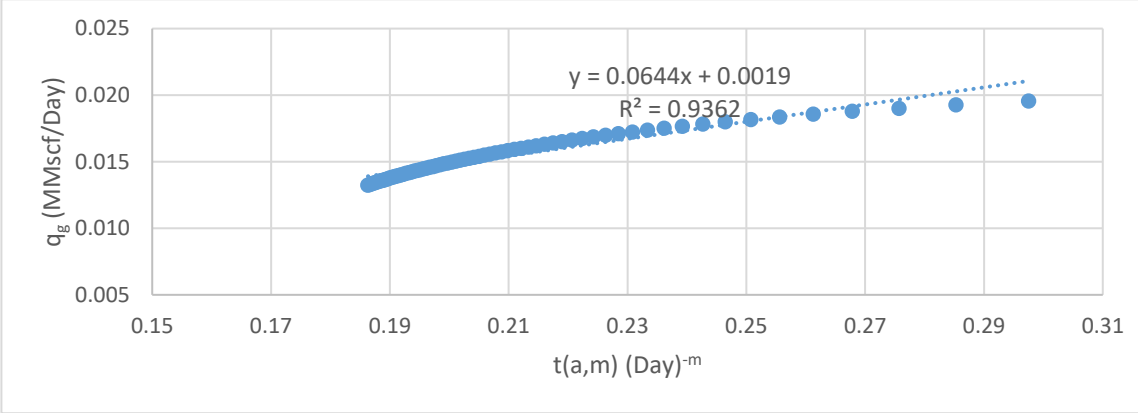

Figure 7.11: Step 3 of Duong model, determination of q_1

A longer duration of historical data improves the calculation of a and m.

Table 7-4: Parameters obtained for Duong model, case 2

Duong's Model parameters	Calculated Value
a	0.5614
m	0.941
q_1 (MMscf/Day)	0.0644

Modified Duong model using 6 months of data

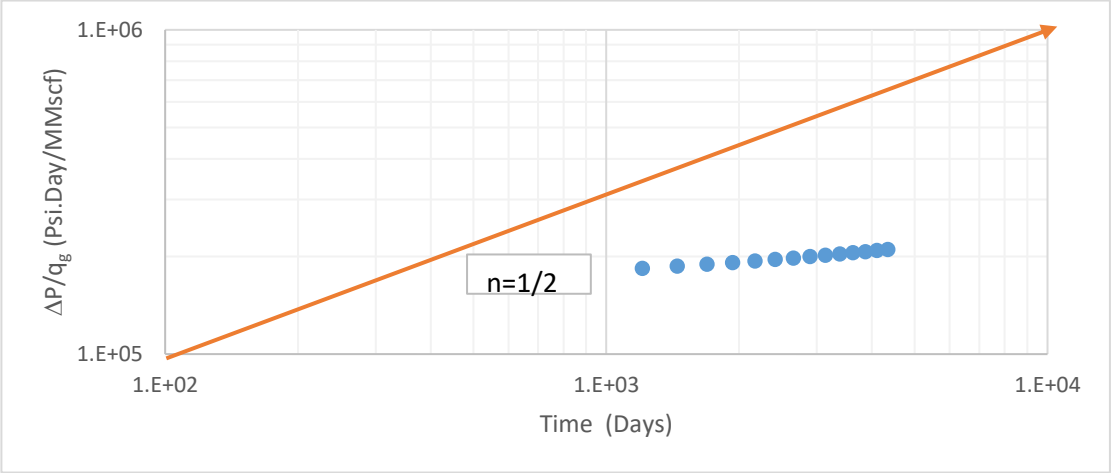

Figure 7.12: Step 2 of modified Duong method, determination of 'n'

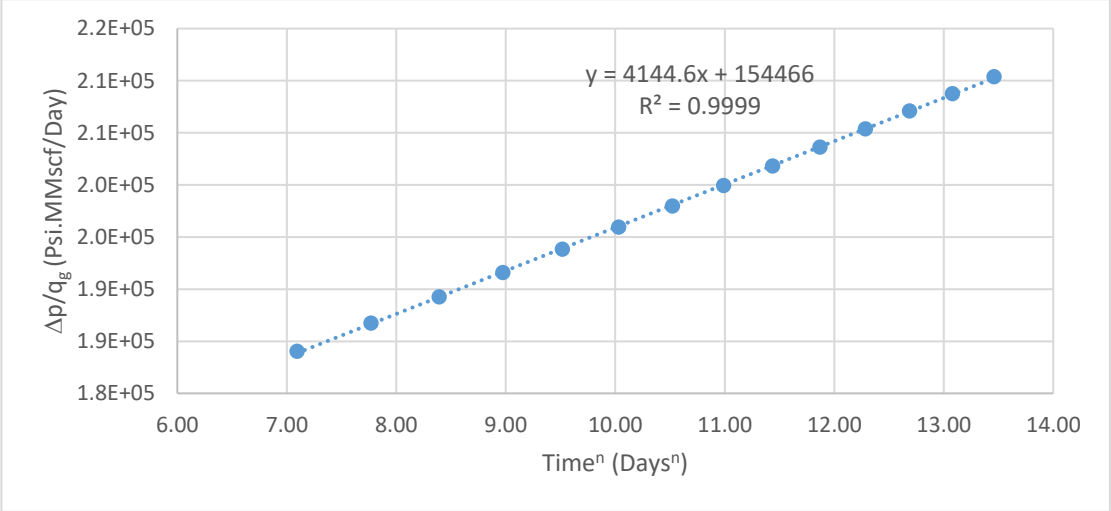

Figure 7.13: Step 3 of modified Duong method, determination of 'm_t' and 'b_tS_f'

Table 7-5: Parameters obtained in modified Duong model, case 2

Modified Duong's Model parameters	Calculated Value
n	$Masked\ due\ to\ fracture\ skin$
m_t	4144.6
b_tS_f	154466

Comparison of prediction results

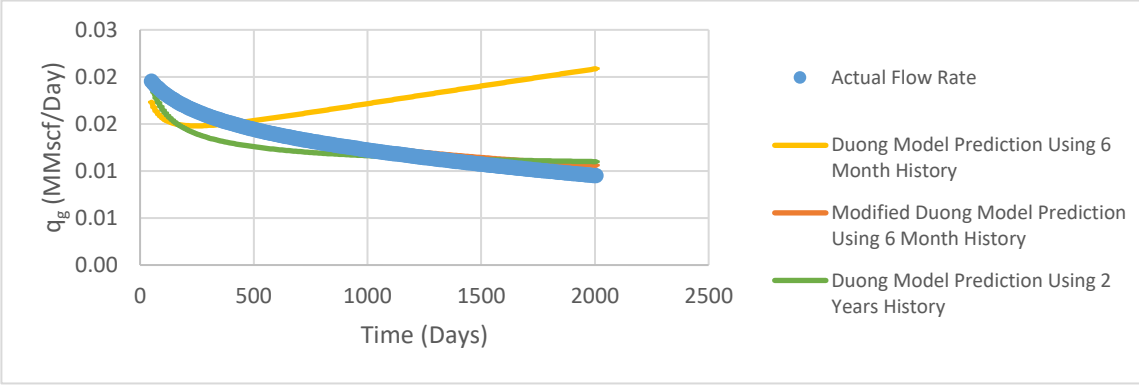

Figure 7.14: Flow rate prediction comparison

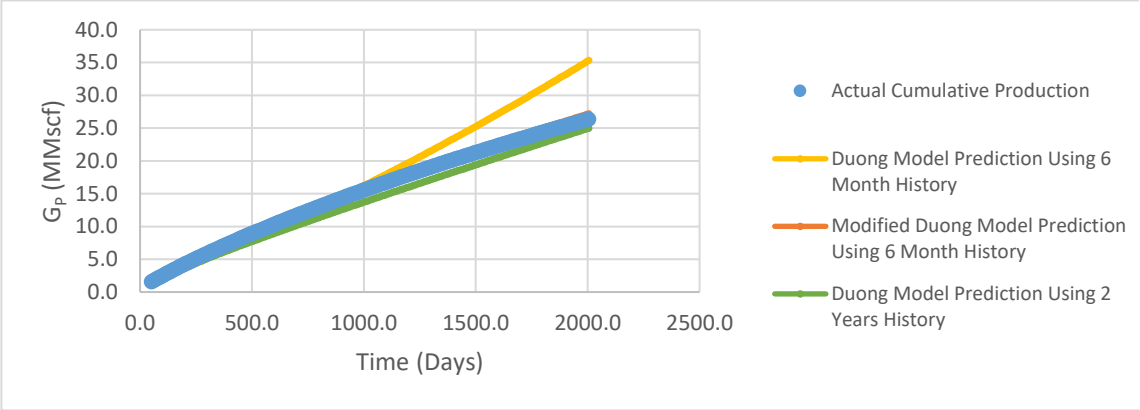

Figure 7.15: Cumulative production prediction comparison

Duong method provides a very poor match for this case with 6 months of data. Predictions from Duong model improve when 2 years of historical data is used, but the results are still not very satisfactory. Modified Duong method seems to be doing well in this case. We believe that the Modified Duong method is doing well in this case is because it accounts for fracture skin in the model.

7.2.3 Case 3: Linear flow, $S_f = 0.5$ and Δp data not available

Duong method using 2 years of data

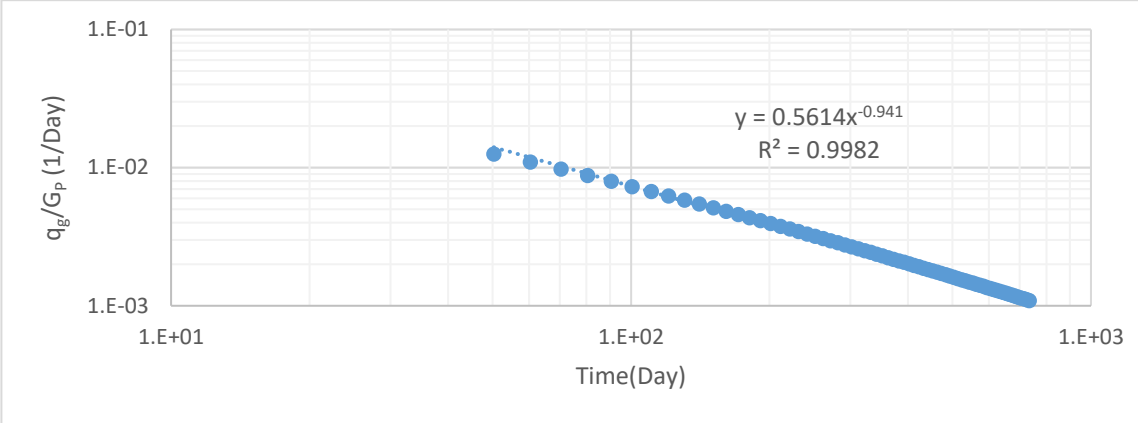

Figure 7.16: Step 2 of Duong method, determination of 'a' and 'm'

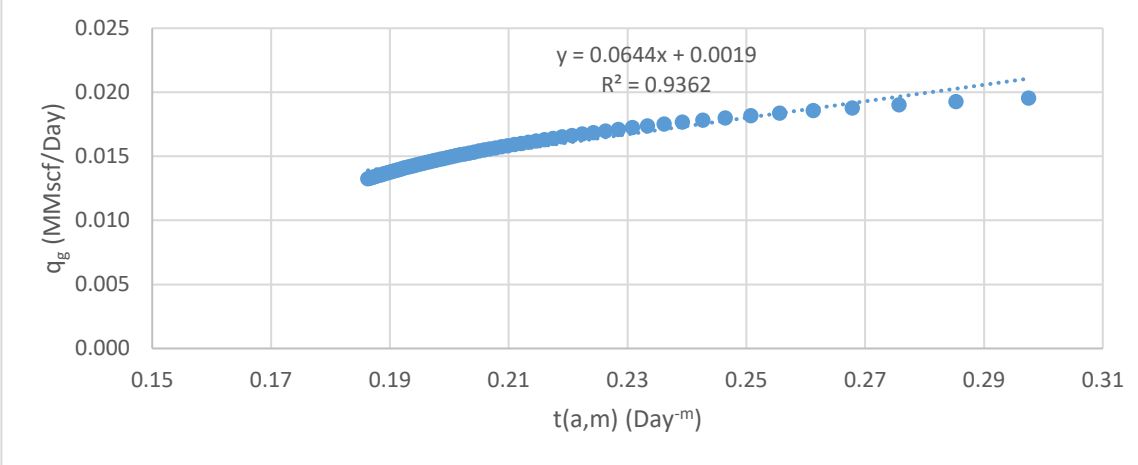

Figure 7.17: Step 3 of Duong method, determination of q_1

Table 7-6: Parameters obtained for Duong model, case 3

Duong's Model parameters	Calculated Value
a	0.5614
m	0.941
q_1 (MMscf/Day)	0.0644

Modified Duong method using 2 years data

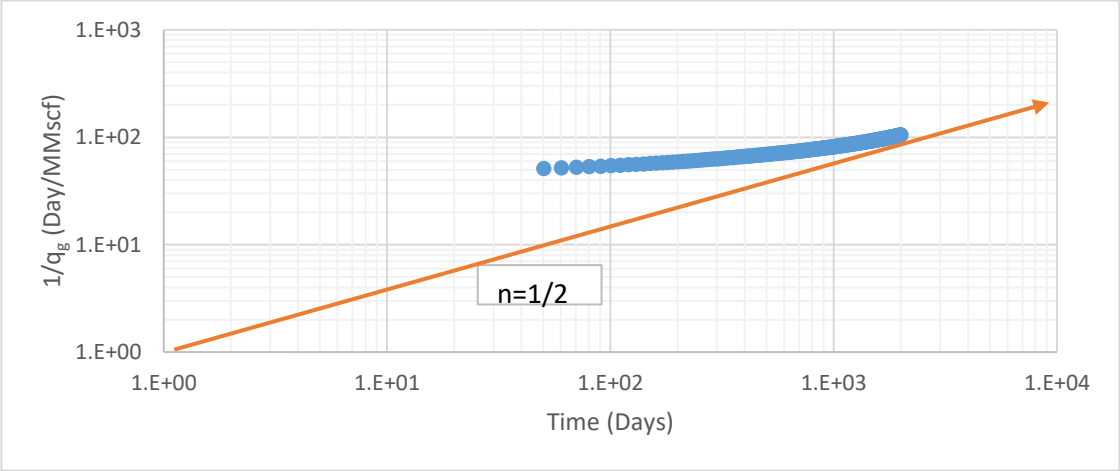

Figure 7.18: Step 2 of modified Duong method, determination of n

Due to presence of fracture skin, n value has been masked.

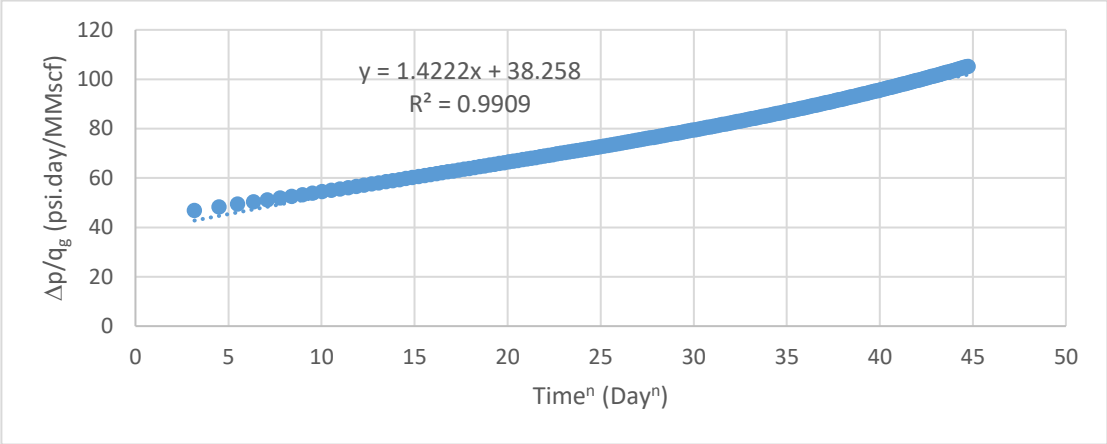

Figure 7.19: Step 3 of modified Duong method, determination of $m_t/\Delta p$ and $b_tS_f/\Delta p$

Table 7-7: Parameters obtained for modified Duong method, case 3

Modified Duong's Model parameters	Calculated Value
n	$Masked\ due\ to\ fracture\ skin$
$m_t/\Delta p$	1.4222
$b_tS_f\Delta p$	38.258

Comparison of prediction results

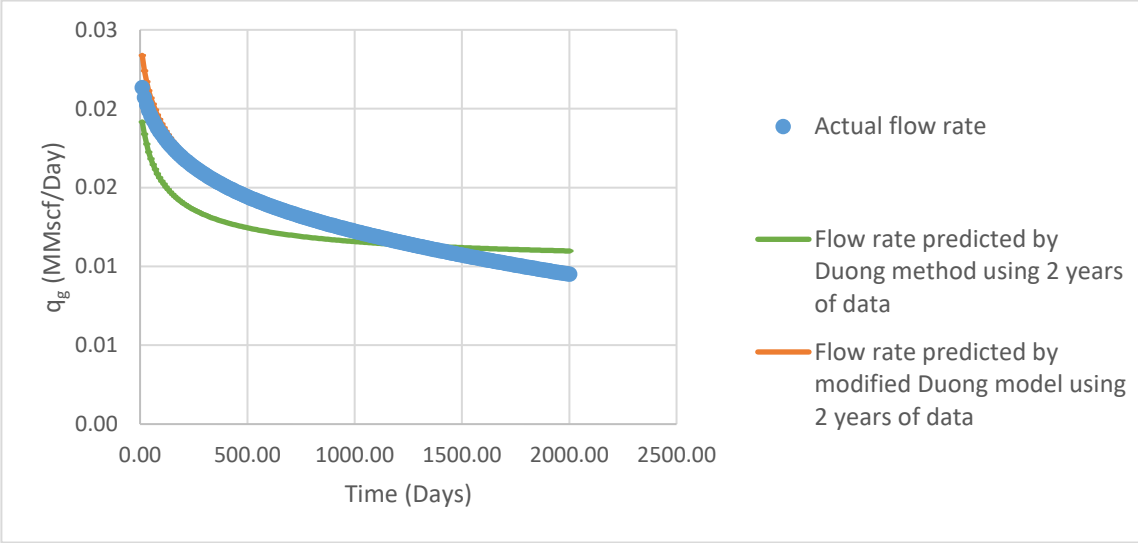

Figure 7.20: Flow rate prediction comparison

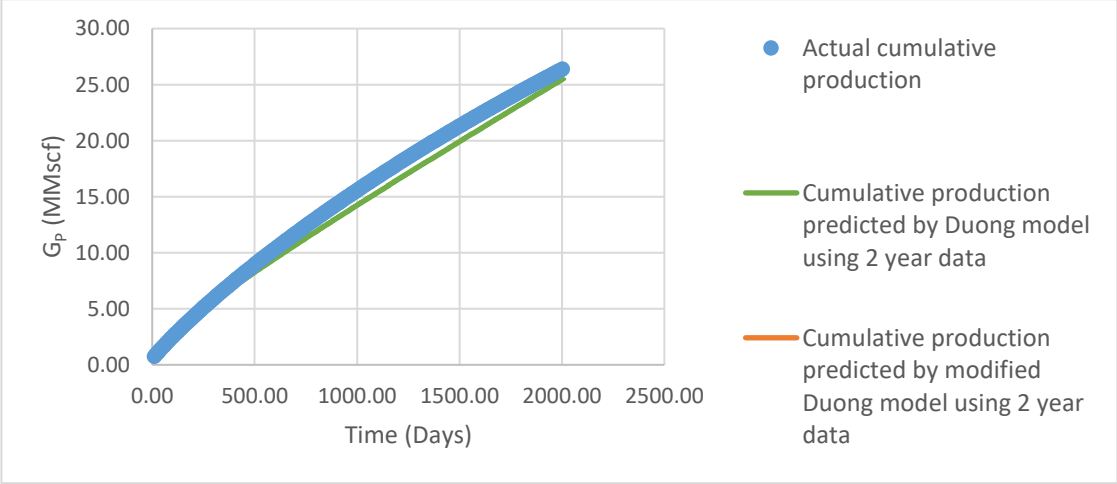

Figure 7.21: Cumulative production prediction comparison

Under constant pressure drawdown, Duong method and modified Duong method remain unaffected by the availability or unavailability of pressure data. Modified Duong method seems to be doing well at predicting flow rate and cumulative production when compared to the Duong method.

7.3 Variable pressure drawdown

Under variable pressure drawdown, the bottomhole pressure is decreased from 2200 psi to 400 psi under a duration of six months. The well was then produced under constant bottomhole pressure for 29.5 years.

Three cases are considered for analysis for variable pressure drawdown case:

Case 4: Variable pressure drawdown, linear flow $S_f = 0$ and Δp data is available,

Case 5: Variable pressure drawdown, linear flow $S_f = 0.5$ and Δp data is available,

and Case 6: Variable pressure drawdown, linear flow $S_f = 0.5$ and Δp data is not available.

Determination of duration of linear flow regime

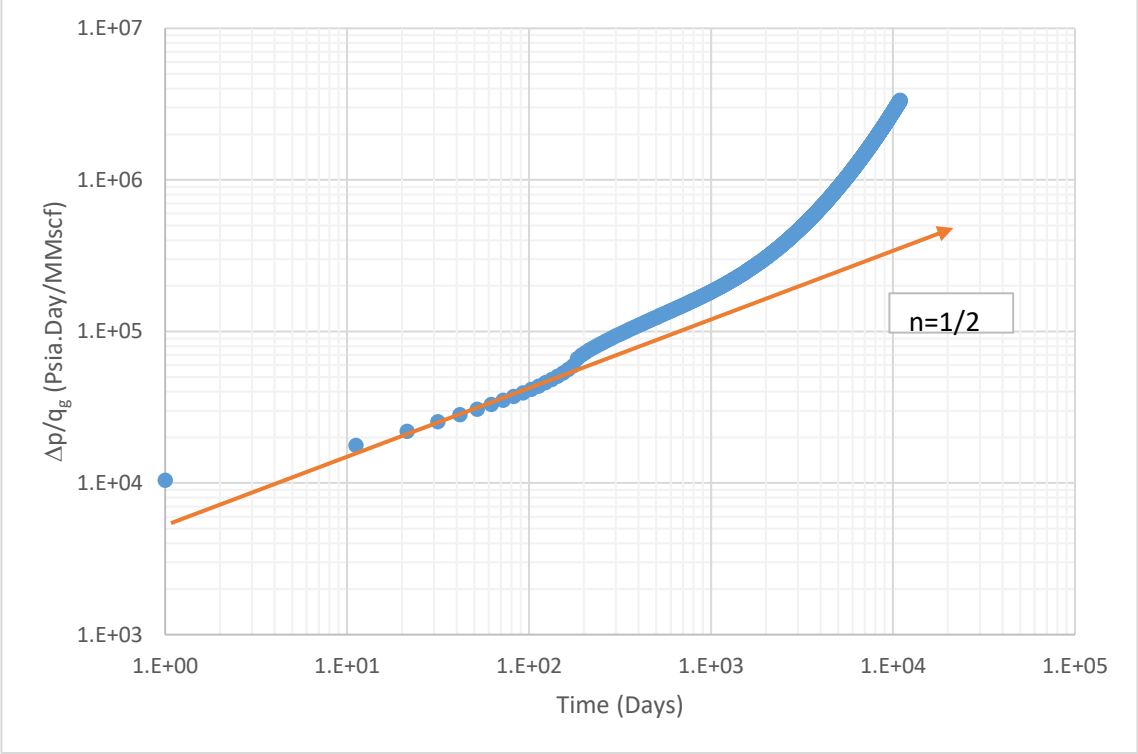

Figure 7.22: Determination of 'n'

From the graph 7.22, it can be seen that the linear flow starts at around 20 days and continues till 1000 days.

7.3.1 Case 4: Linear flow, $S_f = 0$ and Δp value available

Duong method using 6 months of data

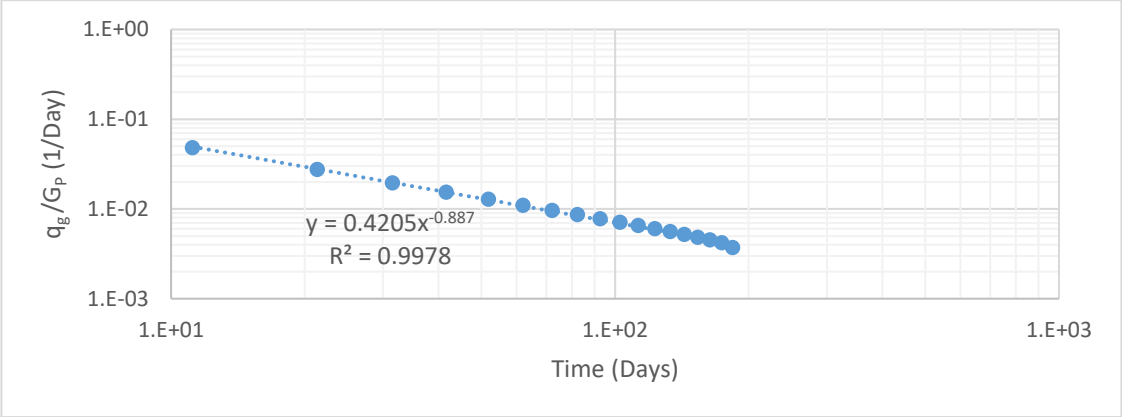

Figure 7.23: Step 2 of Duong method, determination of 'a' and 'm'

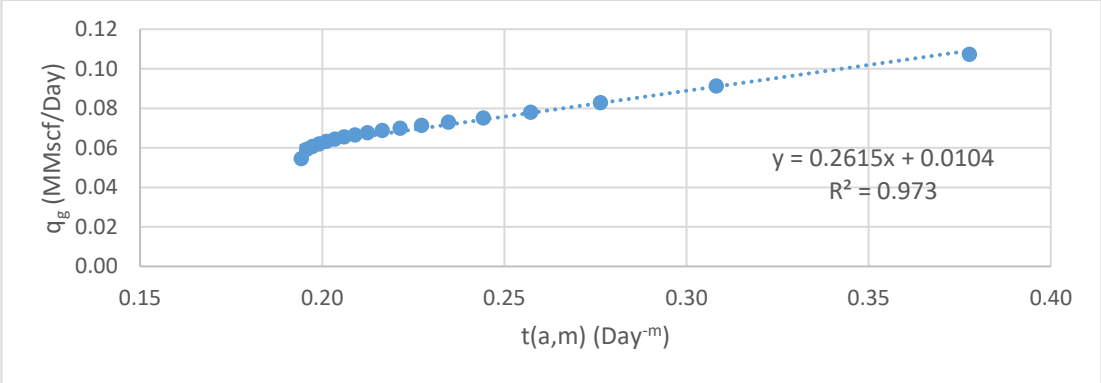

Figure 7.24: Step 3 of Duong method, determination of q_1

Table 7-8: Parameters obtained for Duong method for 6 months of data, case 4

Duong's Model parameters	Calculated Value
a	0.4205
m	0.887
q_1 (MMscf/Day)	0.2615

Duong method using 2 years of data

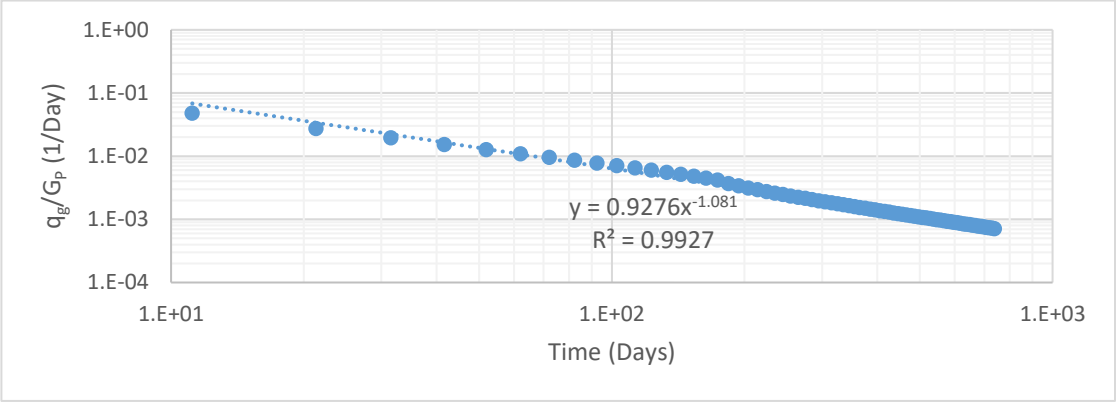

Figure 7.25: Step 2 of Duong method, determination of 'm' and 'bS_f'

When 2 years of production data is used, value of n increases and becomes greater than 1. Also, notice the change in slope of line when pressure switch happens at 180 days.

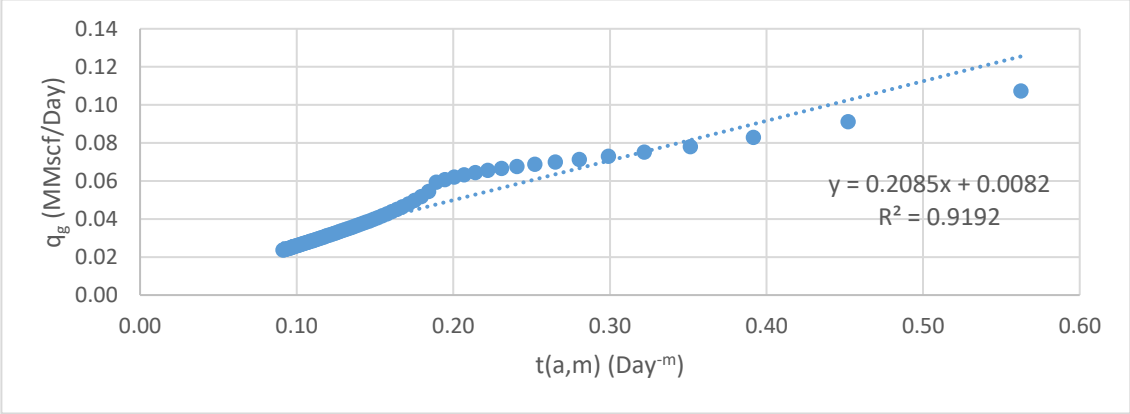

Figure 7.26: Step 3 of Duong method, determination of q_1

Notice the change in slope of line when pressure switch happens at 180 days.

Table 7-9: Parameters obtained for Duong method for 2 years of data, case 4

Duong's Model parameters	Calculated Value
a	0.4205
m	0.887
q_1 (MMscf/Day)	0.2615

Modified Duong method using 6 months of data

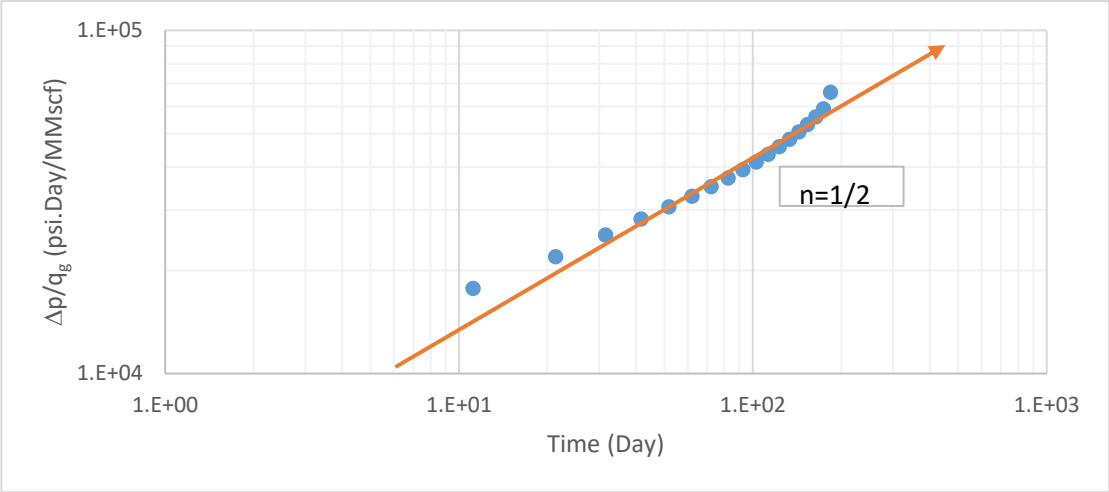

Figure 7.27: Step 2 of modified Duong method, determination of 'n'

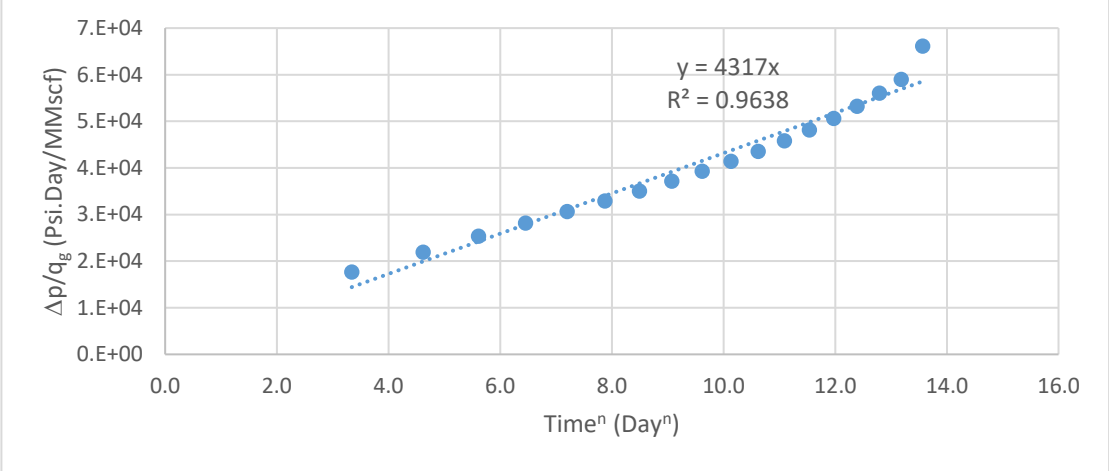

Figure 7.28: Step 3 of modified Duong method, determination of 'm_t' and 'b_tS_f'

Table 7-10: Parameters obtained for modified Duong method with 6 months data, case 4

Modified Duong's Model parameters	Calculated Value
n	1/2
m_t	4317
b_tS_f	0

Modified Duong model using 2 years of data

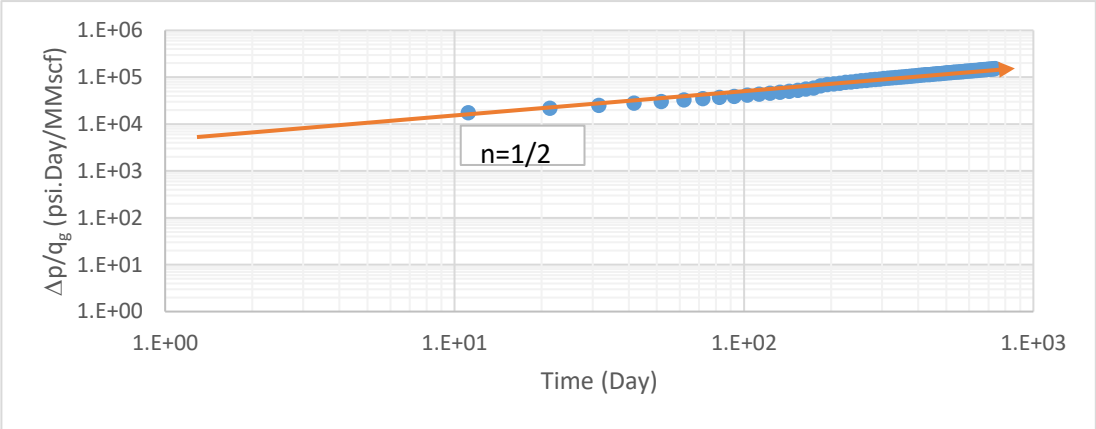

Figure 7.29: Step 2 of modified Duong method, determination of 'n'

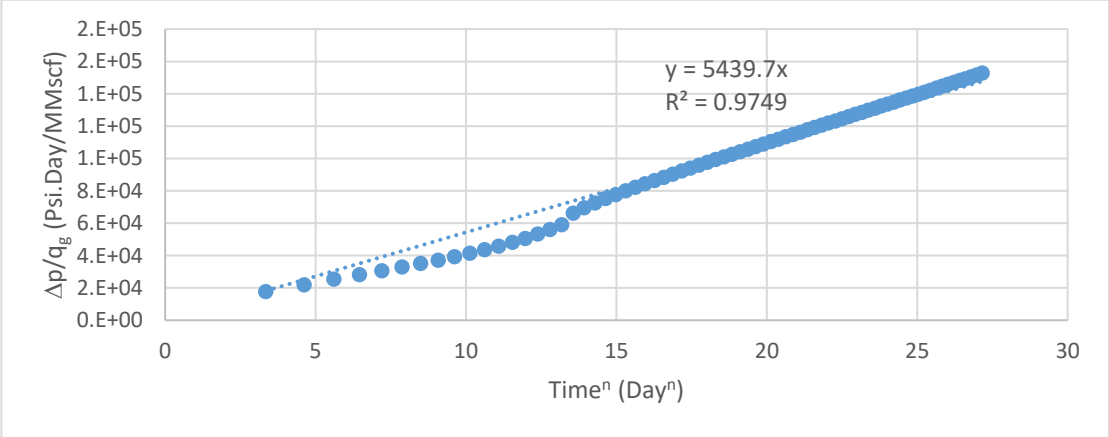

Figure 7.30: Step 3 of modified Duong method, determination of 'm_t' and 'b_tS_f'

Notice the change in slope of line when pressure is switched to constant pressure production at 180 days.

Table 7-11: Parameters obtained for modified Duong method with 2 years data, case 4

Modified Duong's Model parameters	Calculated Value
n	$1/2$
m_t	5439.7
b_tS_f	0

Comparison of prediction results

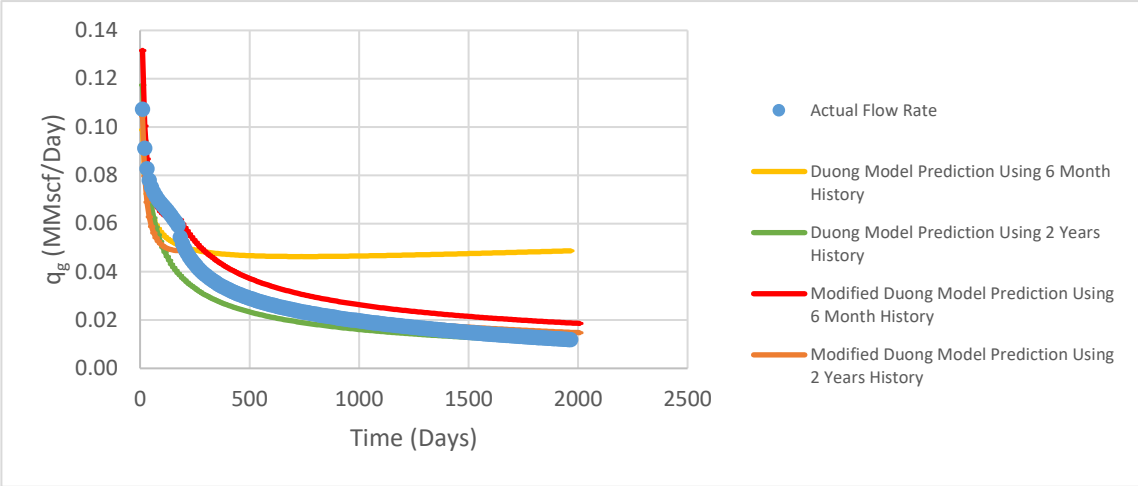

Figure 7.31: Comparison of flow rate prediction results

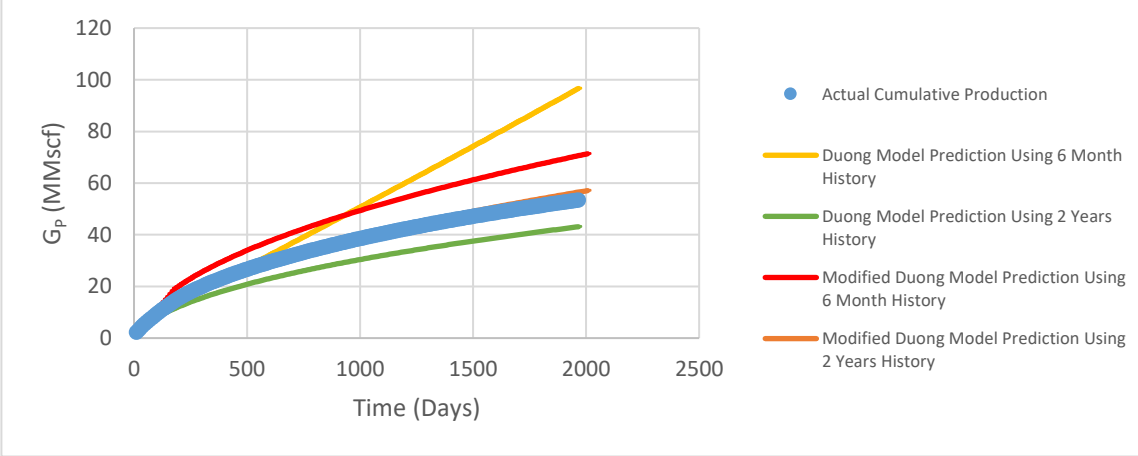

Figure 7.32: Comparison of cumulative production prediction results

Duong method goes completely off track with predicted reserves increasing over the time when only 6 months of historical data is used. Predictions using Duong method improve when the 2 years of data is used to calculate the model parameter. Modified Duong method also does not perform very well with just 6 months of historical data. However, with 2 years of historical data, Modified Duong method gives a perfect match.

7.3.2 Case 5: Linear flow, $S_f = 0.5$ and Δp value available

Duong model using 6 months data

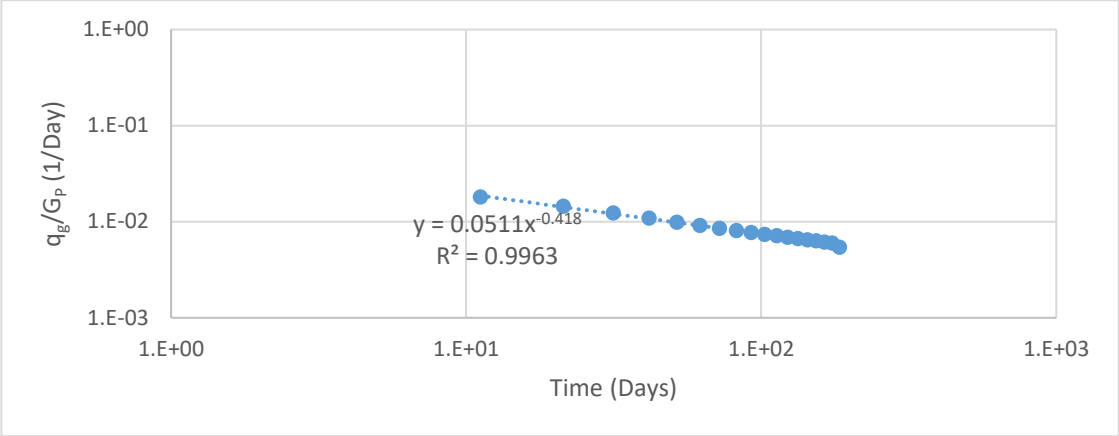

Figure 7.33: Step 2 of Duong method, determination of 'a' and 'm'

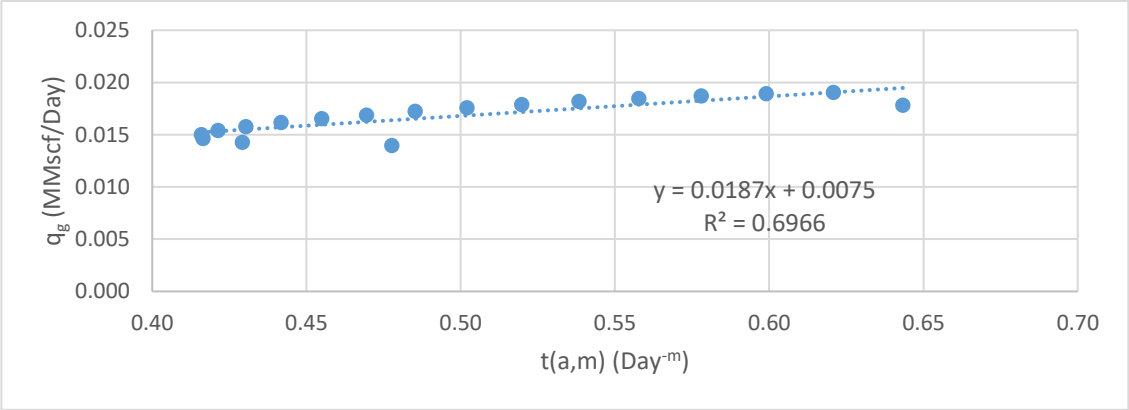

Figure 7.34:Step 3 of Duong method, determination of q_1

$t(a,m)$ becomes non-monotonic as the fracture skin is introduced.

Table 7-12: Parameters obtained for Duong method using 6 months data, case 5

Duong's Model parameters	Calculated Value
a	0.4205
m	0.887
q_1 (MMscf/Day)	0.2615

Duong method using 2 years data

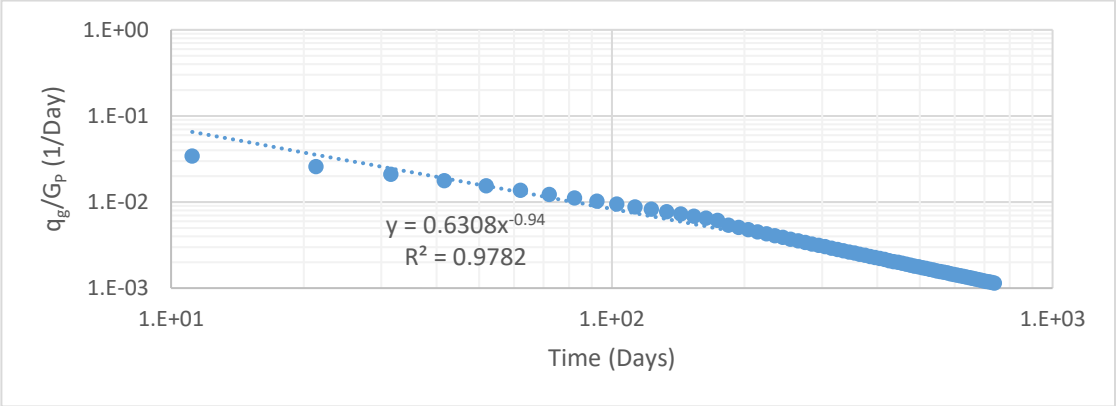

Figure 7.35: Step 2 of Duong method, determination of 'm' and 'bS_f'

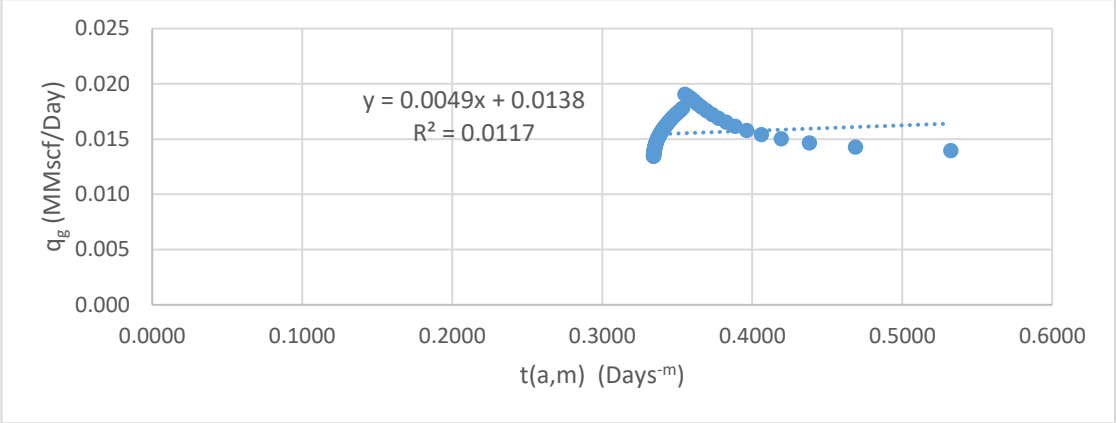

Figure 7.36: Step 3 of Duong method, determination of q_1

Notice the non-monotonic function at time = 180 days when the production is switched to constant pressure production.

Table 7-13: Parameters obtained for Duong method using 2 years data, case 5

Duong's Model parameters	Calculated Value
a	0.6308
m	0.940
q_1 (MMscf/Day)	0.0049

Modified Duong method using 6 months of data

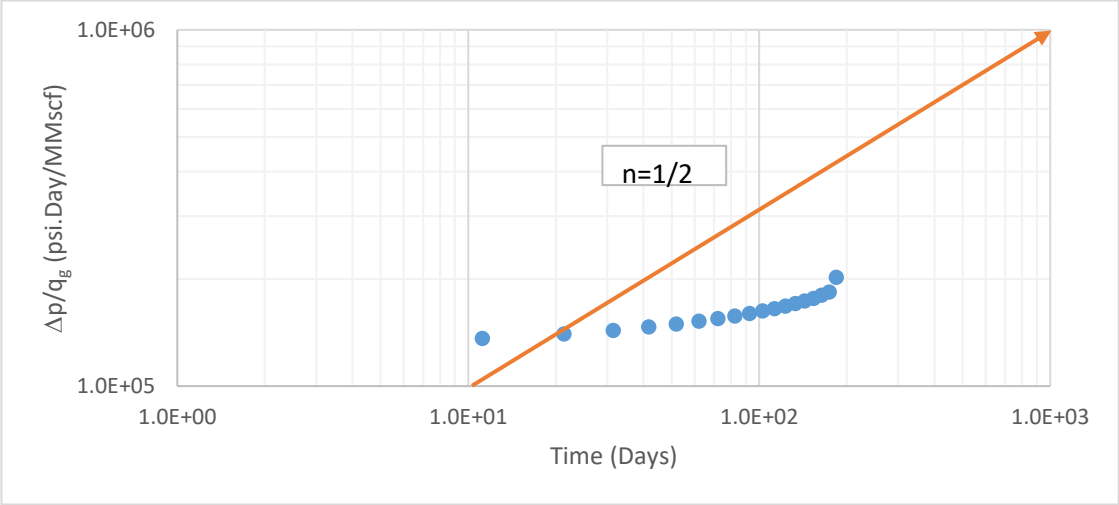

Figure 7.37: Step 2 of modified Duong method, determination of 'n'

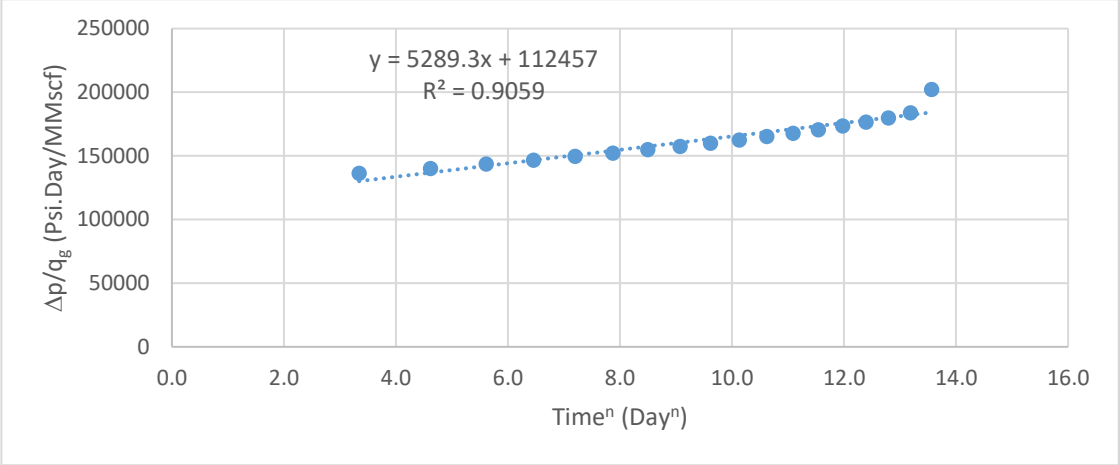

Figure 7.38: Step 3 of modified Duong method, determination of '$m_t t$' and '$b_t S_f$'

Table 7-14: Parameters obtained for modified Duong method using 6 months data, case 5

Modified Duong's Model parameters	Calculated Value
n	$Masked\ due\ to\ presence\ of\ fracture\ skin$
m_t	5289.3
$b_t S_f$	112457

Modified Duong method using 2 years of data

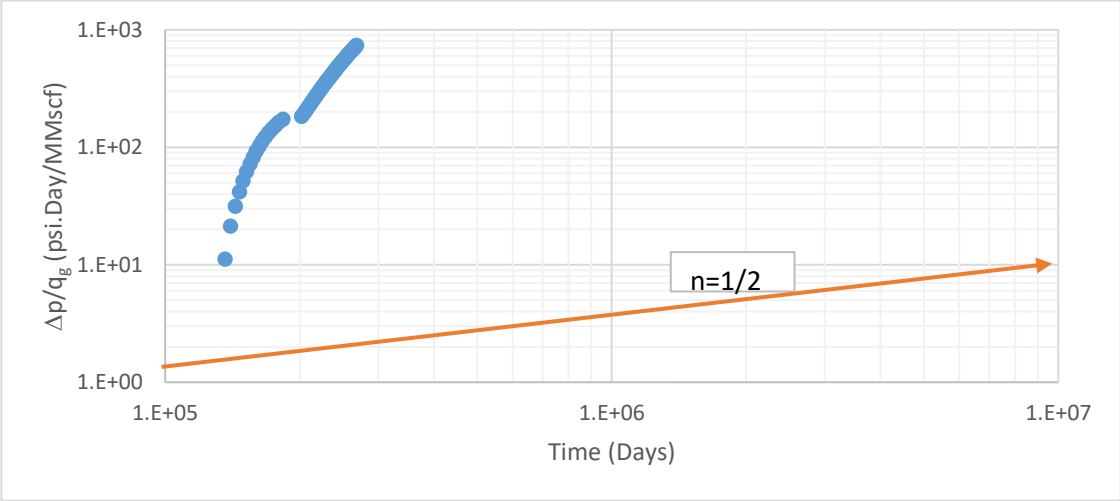

Figure 7.39: Step 2 of modified Duong method, calculation of 'n'

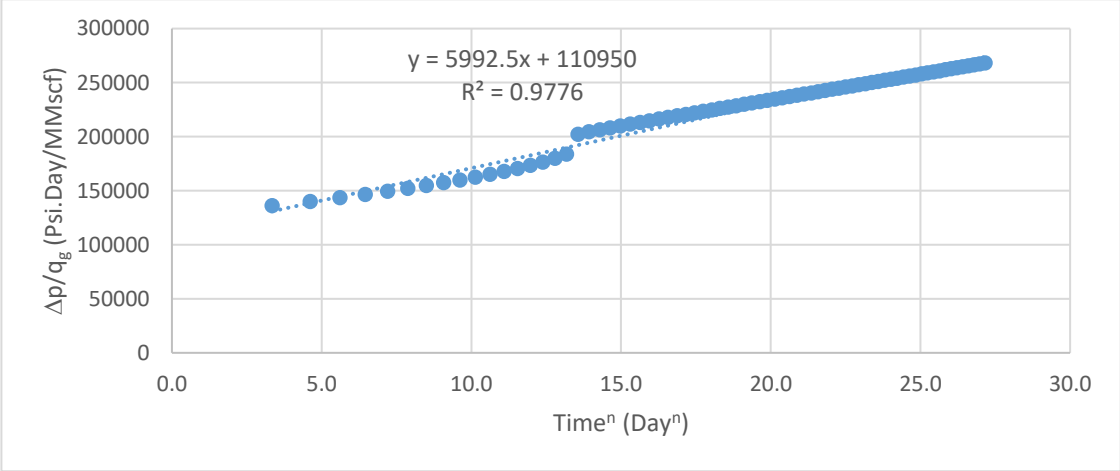

Figure 7.40: Step 3 of modified Duong method, determination of 'm_t' and 'b_tS_f'

Table 7-15: Parameters obtained for modified Duong method using 2 years of data, case 5

Modified Duong's Model parameters	Calculated Value
n	$Masked\ due\ to\ presence\ of\ fracture\ skin$
m	5992.5
bS_f	110950

Comparison of prediction results

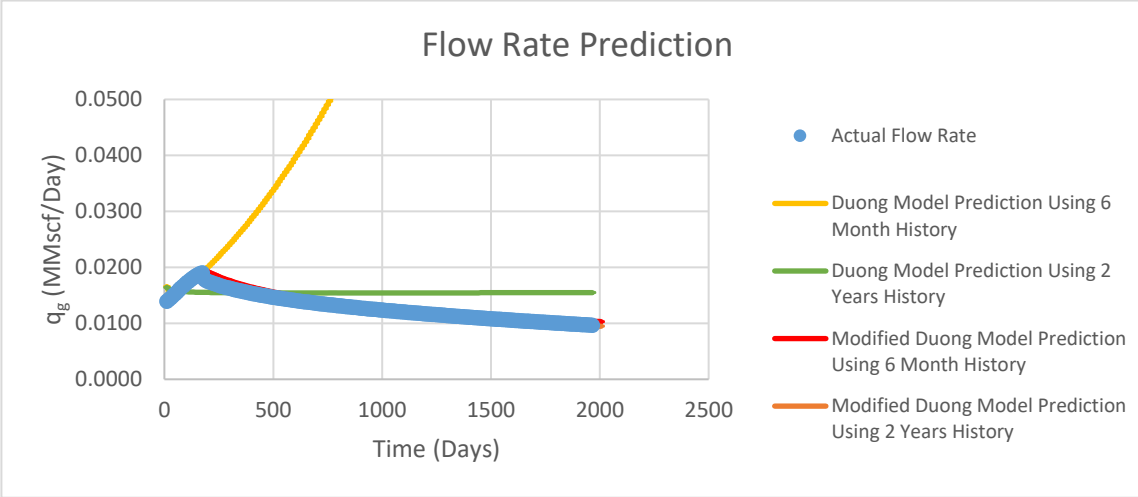

Figure 7.41: Flow rate prediction results

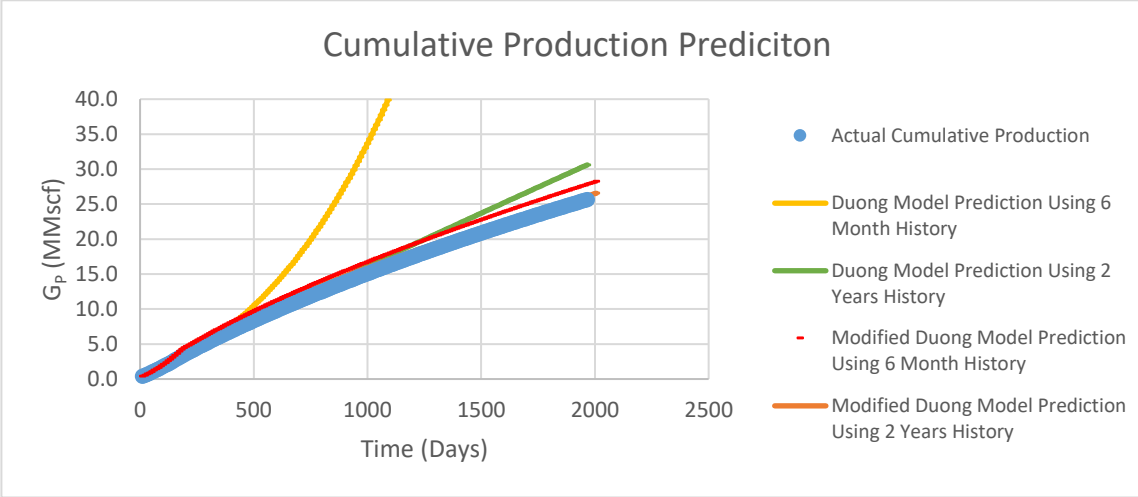

Figure 7.42: Cumulative production prediction results

Duong method is give predictions with reserves increasing over time due to $m < 1$. The prediction using Duong method improves when 2 years of data is used. Modified Duong method seems to be doing well 6 months of data and the accuracy seems to improve further when used with 2 years of data.

7.3.3 Case 6: Linear flow, $S_f = 0.5$ and Δp value not available

Duong model using 2 years of history

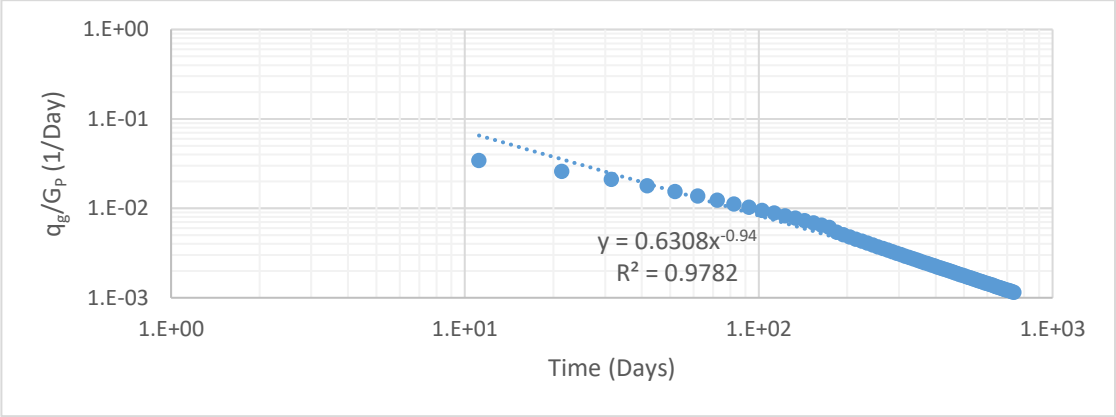

Figure 7.43: Step 2 of Duong method, determination of 'm' and 'bS_f'

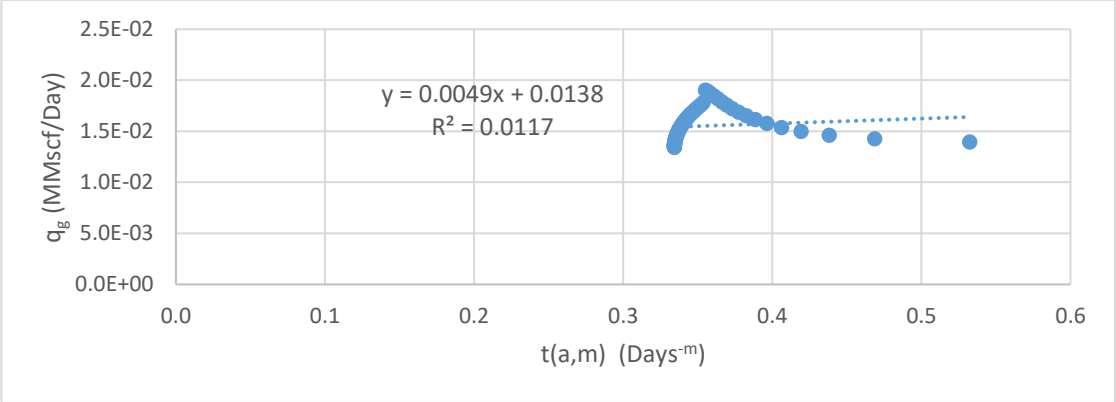

Figure 7.44: Step 3 of Duong method, determination of q_1

We can notice the spike in the data when the pressure is switched to constant pressure production.

Table 7-16: Parameters obtained for Duong method, case 6

Duong's Model parameters	Calculated Value
a	0.6308
m	0.940
q_1 (MMscf/Day)	0.0049

Modified Duong method using 2 years data

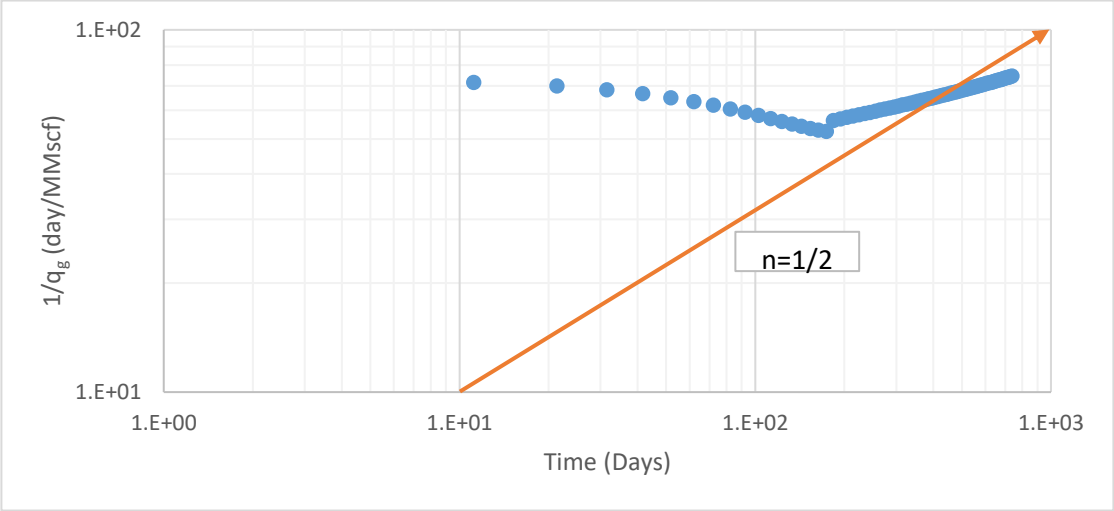

Figure 7.45: Step 2 of modified Duong method, determination of 'n'

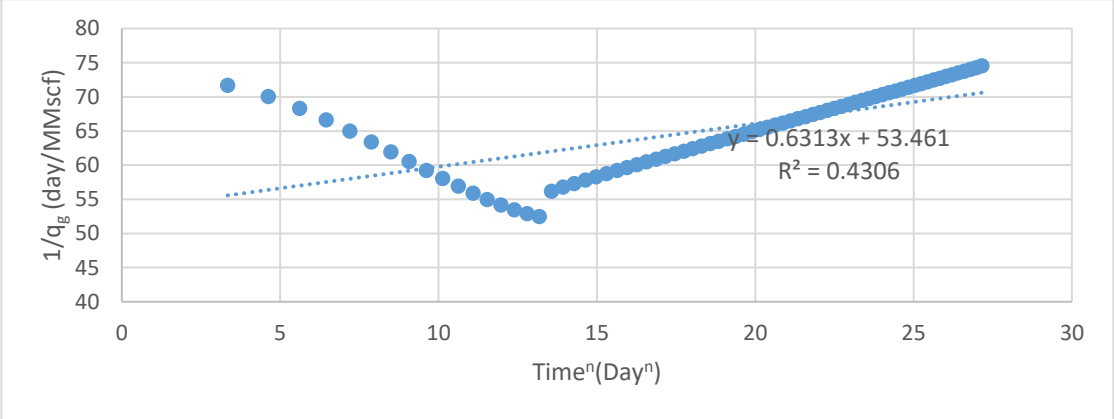

Figure 7.46: Step 3 of modified Duong method, determination of '$m_t/\Delta p$' and '$b_t S_f/\Delta p$'

We can notice the dip in the data when the constant pressure production starts at 180 days.

Table 7-17: Parameters obtained for modified Duong method, case 6

Modified Duong's Model parameters	Calculated Value
n	$Masked\ due\ to\ fracture\ skin$
$m_t/\Delta p$	0.6313
$b_t S_f \Delta p$	53.461

Comparison of prediction results

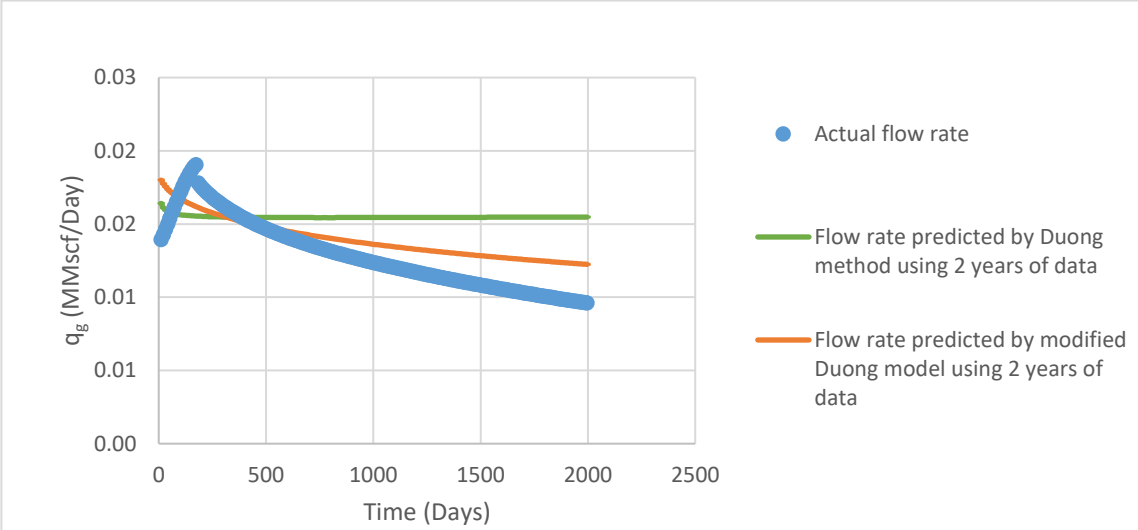

Figure 7.47: Flow rate prediction comparison

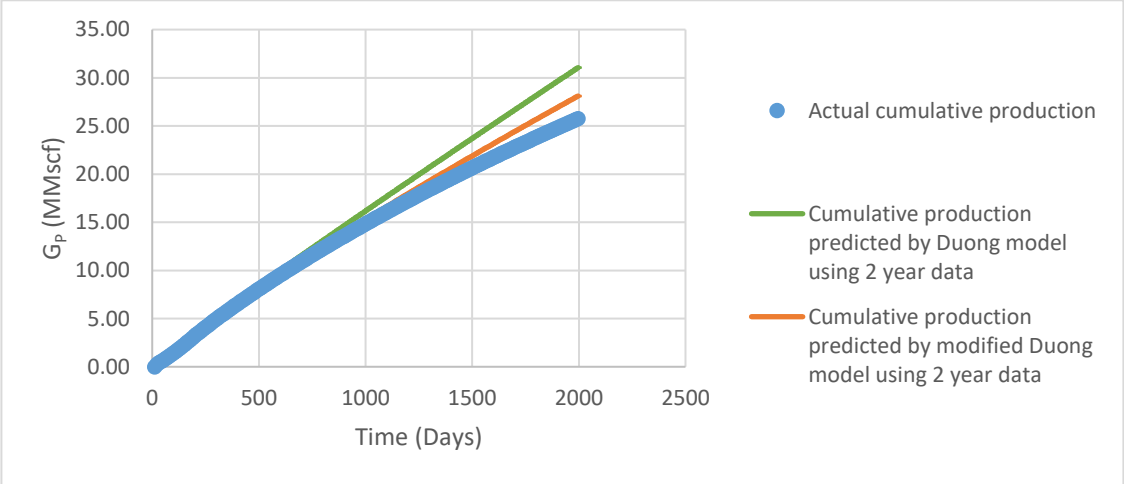

Figure 7.48: Cumulative production prediction comparison

Although, the overall accuracy of flow rate and cumulative volume prediction has reduced in absence of pressure data, Modified Duong method still provides better results than Duong method.

8 Conclusions

- This study presents a critique of the Duong method and explains all of its shortcomings. Most important of these is that Duong model fails to account for the fracture skin in its derivation.
- A modified Duong method is proposed which tries to improve on all the shortcomings of the Duong model.
- Constants determined in the Modified Duong method provide very meaningful insight into the reservoir and fracture properties. The empirical constants used in Duong's method do not provide any such information.
- Both the methods, Duong method and modified Duong method, work best under constant pressure production conditions.
- Presence of fracture skin, and varying bottomhole pressure, both lead to change in the slope of the lines used in the Duong method. This effect is reduced in the case of modified Duong method due to use of normalized pressure. However, in absence of pressure data, modified Duong method also experiences the same issues.
- The accuracy in prediction improves for both the methods when longer historical data is used to calculate the model parameters.
- Various cases analyzed prove that the modified Duong method does a better job at predicting the flow rate and cumulative production when compared to Duong method.

9 Recommendations

- For the purpose of this study, only simulated data and data generated using analytical equation have been analyzed to draw comparisons between Duong method and Modified Duong method. Real field data should be analyzed to see the field applicability of Modified Duong method.
- As it has been shown in this study, the early production data is affected by the presence of fracture skin which masks the actual n value. Modified Duong method should be applied and tested for general values of n to test its validity.
- Duong believes that the value of a and m depends on the permeability and pressure. He states that the value of m will be less than one for tight gas wells and low pressure reservoir. A sensitivity analysis should be carried out to understand the dependence of a and m on the pressure and the permeability of the reservoirs.

References

1. U.S. Energy Information Administration. 2016. Annual Energy Outlook 2016. August 2016, http://www.eia.gov/outlooks/aeo/pdf/0383(2016).pdf (accessed 10 December 2016).
2. Wright, J.D. 2014. *Oil and Gas Property Evaluation*, β test version. Golden, Colorado: Wright Consulting Company, Inc.
3. Arps, J.J. 1945. Analysis of Decline Curves. *Transactions of the AIME* **160** (01): 228-247. SPE-945228-G. http://dx.doi.org/10.2118/945228-G.
4. Fetkovich, M. J., Fetkovich, E. J. and Fetkovich, M. D. 1996. Useful Concepts for Decline Curve Forecasting, Reserve Estimation, and Analysis. *SPE Res Eng* **11** (01): 13-22. SPE-28628-PA. http://dx.doi.org/10.2118/28628-PA.
5. Maley, S. 1985. The Use of Conventional Decline Curve Analysis in Tight Gas Well Applications. Presented at the SPE/DOE Low Permeability Gas Reservoirs Symposium, Denver, Colorado, 19-22 March. SPE-13898-MS. http://dx.doi.org/10.2118/13898-MS.
6. Spivey, J. P., Frantz, J. H., Williamson, J. R., Sawyer, W. K. et al. 2001. Applications of the Transient Hyperbolic Exponent. Presented at SPE Rocky Mountain Petroleum Technology Conference, Keystone, Colorado, 21-23 May. SPE-71038-MS. http://dx.doi.org/10.2118/71038-MS.
7. Lee, W. J. and Sidle, R. 2010. Gas-Reserves Estimation in Resource Plays. *SPE Econ & Mgmt* **2** (02): 86 – 91. SPE-130102-PA. http://dx.doi.org/10.2118/130102-PA.

8. Cinco-Ley, H. and Samaniego-V., F. 1981. Transient Pressure Analysis: Finite Conductivity Fracture Case Versus Damaged Fracture Case. Presented at the SPE Annual Technical Conference and Exhibition, San Antonio, Texas, 4-7 October. SPE-10179-MS. http://dx.doi.org/10.2118/10179-MS.
9. Spivey, J.P. and Lee, W.J. 2013. *Applied Well Test Interpretation*, SPE Textbook Series Vol. 13. Society of Petroleum Engineers.
10. Katz, D.L. 1959. *Handbook of Natural Gas Engineering*. New York: McGraw-Hill Higher Education.
11. Carr, N. L., Kobayashi, R. and Burrows, D. B. 1954. Viscosity of Hydrocarbon Gases Under Pressure. *J Pet Technol* **6** (10): 47-55. SPE-297-G. http://dx.doi.org/10.2118/297-G.